Université de Montréal

Phosphoproteomic study on osmotic shock in *Saccharomyces cerevisiae* over sub-minute and half-hour timescales

par
Seckin Sinan Isik

Département de Biochimie et Médecine Moléculaire
Faculté de Médecine

Mémoire présenté à la Faculté de Médecine
en vue de l'obtention du grade de Maître és Sciences (M.Sc.)
En Biochimie
Option cheminement libre

Décembre 2018

Résumé

La phosphorylation des protéines contribue de manière importante à la régulation cellulaire. Ainsi, les kinases et les phosphatases (KP) sont essentielles à la transduction de signal dans les cellules. Les signaux reçus par la cellule doivent être transmis efficacement pour garantir l'obtention d'une réponse adaptative appropriée. Le suivi de l'activité de phosphorylation des protéines nous aide à mieux comprendre comment les cellules fonctionnent. Dans notre étude, nous avons exposé *Saccharomyces cerevisiae* à une osmolarité élevée, soit 0,4 M de NaCl, ce qui a provoqué un choc hyperosmotique. La phosphorylation des protéines a été mesurée à l'aide d'une technique de spectrométrie de masse appelée ``Marquage en culture cellulaire avec des acides aminés dotés d'isotopes stables (SILAC)'. Il s'agit d'une technique quantitative de protéomique qui permet de comparer des cellules exposées au choc hyperosmotique à un groupe contrôle où les cellules n'ont pas subi ce choc. Cette comparaison entre les deux groupes nous permet de déduire une régulation dynamique des protéines spécifique au stimulus appliqué. Nous avons utilisé deux échelles de temps, la première inférieure à une minute et la seconde de 30 minutes, pour examiner les effets du choc osmotique chez *S. cerevisiae*.

Dans ce mémoire, j'ai examiné la voie métabolique MAPK-Hog1 au cours de la demi-heure de mesure et l'ai comparée aux mesures prises lors de l'échelle inférieure à la minute, laquelle ayant été publiée précédemment par Kanshin & Bergeron-Sandoval *et al*., 2015 [26]. De plus, les données complètes contenaient 161 phosphopeptides dynamiques provenant de 100 protéines distinctes présentes lors des deux échelles de temps. Les phosphopeptides dynamiques découverts furent également comparés à une autre étude phosphoprotéomique ayant utilisé le stress froid / chaud comme stimulus (Kanshin *et al.,* 2015 [25]). Il y avait des chevauchements remarquables des phosphopeptides kinétiques observés lors des chocs osmotiques et en particulier ceux observés lors du stress thermique. Cela nous a mené à examiner la possibilité d'une implication de TORC1 & 2 dans le processus

d'osmoadaptation. De plus, les cellules arrêtent temporairement leur cycle cellulaire lors de ce processus d'osmoadaptation. Conformément à cette observation, 68% des protéines impliquées dans la transition G1 / S ont subi des modifications de la phosphorylation, lesquelles reflétant peut-être leur régulation, au cours des 30 premières minutes de choc osmotique.

Les kinases et les phosphatases sont connues pour fortement se réguler les unes les autres. Un réseau de KP actives interconnectées a révélé que Hog1 était la kinase la plus connectée dans les mesures à l'échelle de temps inférieure à la minute alors que Cdc28 était la plus connectée lors de l'échelle de temps d'une demi-heure. Cela est indicatif du mécanisme par lequel les cellules s'adaptent à une osmolarité élevée. Par exemple, Hog1 est responsable de la détection rapide et de l'adaptation, et Cdc28, de l'arrêt et de la régulation du cycle cellulaire.

En résumé, j'ai soutenu qu'il était possible d'identifier des phosphopeptides dynamiques spécifiques à un stimulus dans l'échelle de temps d'une demi-heure. J'ai comparé les phosphopeptides dynamiques de l'échelle de temps inférieure à la minute à l'échelle de 30 minutes et j'ai examiné les processus biologiques qui jouent un rôle dans le processus d'osmoadaptif.

Mots-clés: phosphosites fonctionnels, réseau des kinases-phosphatases, Saccharomyces cerevisiae, structure hiérarchique des réseaux, cycle cellulaire, osmoadaptif, cible de la rapamycine chez les mammifères, système des MAP kinases.

Abstract

Protein phosphorylation is an important cellular regulatory mechanism. Kinases and phosphatases (KP) are vital for the signalling transductions in cells. Signals received by the cell must be transmitted effectively to ensure an appropriate adaptive response is achieved. Monitoring the phosphorylation activity on proteins helps us gain a better understanding to how cells work. In our study we have exposed *Saccharomyces cerevisiae* to high osmolarity using 0.4M NaCl, and caused a hyper osmotic shock. Protein phosphorylation was measured using a mass spectrometry technique called Stable Isotope Labeling by/with Amino acids in Cell culture (SILAC). This is a quantitative proteomic technique that allows the comparison between cells that are exposed to NaCl and a control group, where cells are not exposed to NaCl. This comparison between the two groups allows us to deduce dynamic regulation of proteins specific to the stimulus applied. We have used a sub-minute and a half-hour timescales to examine the effects of osmotic shock in *S. cerevisiae.*

In this memoir, I have examined the MAPK-Hog1 pathway during the half-hour timescale and have compared it to the sub-minute timescale, which was previously published in Kanshin & Bergeron-Sandoval et al., 2015 [26]. Moreover, the entire data had 161 dynamic phosphopeptide from 100 unique proteins that were present on both timescales. Dynamic phosphopeptides were also compared to another phosphoproteomic study that had used cold/hot stress as a stimulus (Kanshin et al., 2015 [25]). There were remarkable overlaps between osmotic shock and in particular heat stress. This led us to examine the possibility that TORC1&2 involvement in the osmoadaptation process. Furthermore, cells temporarily stop cell cycling during the osmoadaptation process. Consistent with this observation, 68% of the proteins involved in the G1/S transition underwent changes in phosphorylation, perhaps reflecting their regulation, during the first 30 minutes of osmotic shock.

Kinases and phosphatases are known to heavily regulate themselves. A network of interconnected active KPs revealed Hog1 to be the most connected kinase in the sub-minute timescale, and Cdc28 to be the most connected in the half-hour timescale. This is indicative of how cells adapt to high osmolarity; Hog1 being responsible for the fast sensing and adaptation, and Cdc28 for stopping and regulating the cell cycle.

In summary, I have argued that it is possible to extract dynamic phosphopeptides that are stimulus-specific within the half-hour timescale. I have compared dynamic phosphopeptides from the sub-minute timescale to the half-hour timescale and have examined biological processes that play a part in the osmoadaptive process.

Keywords: dynamic phosphorylation, kinase-phosphatase network, Saccharomyces cerevisiae, network hierarchical structure, cell cycle, osmoadaptation, mammalian target of rapamycin, mitogen-activated protein kinase

List of Content

3- Results

4- Discussion

5-Conclustion and Perspective

6-References

List of Abbreviations

ACN	acetonitrile
ATP	adenosine triphosphate
BCA	bicinchoninic acid assay
CME	clathrin-mediated endocytosis
CWI	cell wall integrity pathway
DLC	dimensional liquid chromatography
DNA	deoxy ribonucleic acid
ESI	electrospray ionization
FDR	false discovery rate
FC	fold change
Fc_{max}	maximum fold change
Fc_{tmax}	time at maximum fold change
GFP	green fluorescent protein
HOG	high osmolarity glycerol
HPLC	high-performance liquid chromatography
KP	kinase phosphatase
LC	liquid chromatography
LFM	low fluorescence medium
MAPK	mitogen-activated protein kinase
MAPKK	mitogen-activated protein kinase kinase
MAPKKK	mitogen-activated protein kinase kinase kinase
MBF	MCB-binding factor
MS	mass spectrometry
mRNA	mature ribonucleic acid
m/z	mass-to-charge ratio
OD	optical density
ORF	open reading frame
PBS	phosphate buffered saline
PKA	protein kinase A
PPI	protein-protein interaction
RFP	red fluorescent protein
RNA	ribonucleic acid
SBF	SCB-binding factor
SCX	strong cation exchange
SILAC	sable isotope labeling with amino acids in cell culture
STRE	stress response element

TFA	trifluoroacetic acid
TOR	target of rapamycin
TORC1/2	target of rapamycin complex 1 / 2

List of Digital Tables

ix

List of Figures

Acknowledgements

I would like to thank my supervisor Prof. Stephen W. Michnick. I do not think there are many researchers out there who value interdisciplinary work as much as Steve. This was the reason how I begun pursuing my ambitions in science in his laboratory. I sincerely appreciate the opportunity you have given me in your lab, and also the generous amount of time to complete my master's memoir.

I would like to thank my committee members Prof. Pascal Chartrand, Dr. Katherine L.B. Borden and Dr. Eric Lecuyer for challenging me and broadening my understanding in molecular biology during my pre-doctoral exam. I would like to take the opportunity to thank Dr. Bram Stynen for teaching me invaluable knowledge in the laboratory, years of scientific discussions and being a friend, Dr. Cornelia Zorca for her guidance during my pre-doctoral exam and my master's memoir, and Dr. Durga Sivanesan for helping me with a great many things during my first years in the laboratory, and Louis-Philippe Bergeron Sandoval for all the many discussions in science. I would also like to thank my special colleagues, Lidice, Lara, Nozhat, Abdellali, Arturo, Pascal, Samir, Diala, Luz, Emmanuelle, Alessandra, Isabel, Poonam and Shelly.

Would like to also thank Sylvie Beauchemin, Linda D'Astous, Elaine Meunier and Kathie Gierka for making bureaucracy feel manageable, and my past and present laboratory managers Jean-Francois Paradis, Jacqueline Moreno Kovarzyk and Philippe Garneau.

Finally, I would like to thank my Family and Marie-Helene Lamarche for supporting me during these years.

1 Introduction

Earth provides an ever-fluctuating environment for organisms that inhabit it. Nutrition, temperature, pH, salinity are environmental properties that constantly change and force organisms to either adapt or perish. Yeast cells are single-cell organisms that live freely in nature that have a remarkable capacity for adaptation. Adaptation is a fundamental feature for survival. Mechanisms involved in adaptation include sensing external changes, which in turn trigger cellular response mechanisms that help cells cope with these environmental challenges. Yeast response mechanisms to the extracellular changes often begin at the plasma membrane, where there are sensors that detect stimuli. Through dedicated signalling pathway, the signal is then relayed within the cell, resulting in an adaptive response. The cellular response to stress generally increases overall cellular fitness, growth and proliferation.

Broadly, a stress is any stimulus that disrupts cellular homeostasis. For cells to respond to stress swiftly and adequately there are few key signalling features. Some of these include: signal fidelity, redundant or alternative pathways involved in the relay of the signal, and in some cases, robustness in response, which is a consequence of feedback mechanisms that integrate signals. Phosphorylation kinetics obtained by mass spectral analysis combined with readily available protein-protein interaction data are crucial for elucidating some of the triggered pathways in the osmoadaptation of *Saccharomyces cerevisiae* (budding yeast).

1.1 Osmotic homeostasis and water

For all eukaryotic cells one critical physical parameter that requires regulation, that is crucial for optimal biochemical reactions, is the ratio between available and bound water within the cell [1]. Water activity is the measure of available water. In regards to the level of available water in the cytosol, there are two extreme cases. First, a sudden increase in intracellular water activity, which results in the increase of cell size, known as hypo-osmotic shock. Second, the sudden decrease in intracellular water activity, which results in the shrinkage of cell size that is known as hyper-osmotic stress.

During a hypo-osmotic shock a force is generated due to the decreased cytoplasmic water potential, which in turn drives extracellular water into the cytosol. This force is

counteracted with the increase of cellular turgor pressure caused by the entered water. Cells sense the excess of turgor pressure and reduce it by an aquaglyceroporin Fps1, a transmembrane protein, that acts like a valve expelling intracellular glycerol [2]. In the case of hyper-osmotic shock, the water activity in the cytosol is higher than its surrounding; an outward force is generated due to the decreased water potential of the extracellular environment, pushing the water out from the cell. Cells sense the loss of water and they adapt to this change by synthesizing cytosolic glycerol. This increases intercellular turgor pressure and reduces intracellular water potential due to the increase in osmolytes. The reduced water potential results in drawing back some of the water from the extracellular space. In addition, Fps1 is activated to fine balance intracellular turgor pressure. Cells that have adapted can resume growing and proliferating [1].

For example, yeast cells growing on grapes could suddenly be exposed to high sugar levels as grape ruptures due to external forces. As a result, these cells experience a hyperosmotic shock, causing a rapid outflow of water leading a cell to shrink. Or the opposite may occur; cells cohabiting on a drying grape could suddenly be drenched in a rain shower that results in a hypo-osmotic shock. This causes a rapid influx of water into the cytosol leading the cell to swell, and hence this also increases turgor pressure. These two cases can be so extreme that a yeast cell may end up relying on its cell wall to prevent it from bursting [1]. In addition to this, there is yet another process where a stress similar to osmotic shock can be triggered. In the production of some beer and wine fermentations, the ethanol concentration can reach up to 20% of the volume. This ethanol permeates back into cells affecting the hydration of biomolecules, resulting in a water stress that is similar to hyperosmotic shock [3][4]. As a result, yeast cells need to be resilient to fluctuating environmental conditions.

The initial interest in elucidating the molecular mechanisms of yeast osmoadaptation was a result of wanting to improve the performance of yeast strains in various applications in industry. In addition to the fermentation industry, another particular interest was to improve food preservation through dehydration by inducing a low water activity in yeast cells. However, in 1993, this research field gained a wider scientific interest with the discovery of a mitogen-activated protein kinase (MAP kinase) cascade. This is a conserved eukaryotic signalling transduction module that is present from fungi to humans [5][6].

1.2 The high osmolarity glycerol pathway (HOG)

Cells use signal transduction pathways to detect and respond to changes in environmental conditions. These environmental changes are constantly sensed and evaluated by the Mitogen Activated Protein Kinase (MAPK) signalling module. This module consists of three sequential kinases: a MAPK Kinase Kinase (MAPKKK), MAPK Kinase (MAPKK) and MAPK [7]. Budding yeast is able to recognize and respond to its environment through five functionally distinct MAP kinases pathways: the cell wall integrity pathway (CWI), two osmoregulation pathways, the pheromone response pathway, the filamentation pathway, and the sporulation-meiosis pathway [6]. Each of these pathways have their unique MAPK, MAPKK and MAPKKK. The MAPK components for each pathway have a high degree of homology with each other. It is thought that this homology arose by gene duplication events early in eukaryotic evolutionary biology. These pathways can also control cell fate decision depending on nutrition, pheromone conditions and general stress levels.

In the case of high extracellular osmolarity there are two distinct pathways that converge on the MAPKK Pbs1, that in turn activate the MAPK Hog1. Phosphorylation of Hog1 at residues T174 and Y176 activate it and causes it to translocate to the nucleus. This translocation activates transcription factors triggering the cellular osmoadaptation process [8],[9],[10],[11]. These residues are within the TGY motif, which is conserved from yeast to humans. Upstream of Hog1, the MAPKK Pbs1 is regulated at residues S514 and T518, by Ste11 and Ssk2/Ssk22, which belong to two different osmosensor branches. Signals from the membrane originate and reach Hog1 via two distinct osmosensor branches. These branches are called the Sho1 branch, and the Sln1 branch. The Sln1 branch is a sub-branch that was first known in prokaryotes [12]. Sln1 is essential for yeast homeostasis and its deletion, *SLN1,* causes cells to be inviable [13]. Sln1 is a transmembrane histidine phosphotransfer kinase that is active under iso-osmotic conditions and inactive upon hyperosmotic shock. It contains an extracellular sensor domain and an intercellular histidine kinase domain that auto phosphorylates itself at residue H576. This phosphate is then transferred to residue D1144 on Sln1 and is then relayed to residue H64 on an intermediate sensor protein Ypd1. Ypd1 then transfers the phosphate to Ssk1 at residue D554. This D554 phosphorylation prevents it from interacting

with the MAPKKK, Ssk2/Ssk22. This kind of phosphorylation is referred to as two-component signalling machinery, and it does not involve serine/threonine/tyrosine phosphorylation (Figure 1) [14].
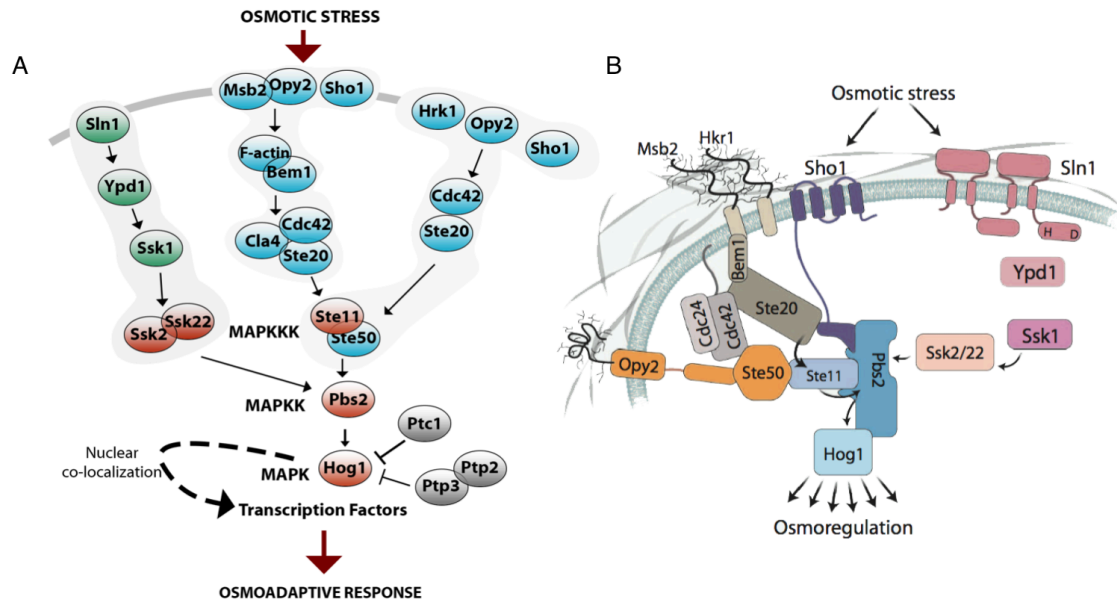
Figure 1: The schematic model and the layout of the high osmolarity glycerol pathway in *S. cerevisiae.*
(A) The schematic represents the direction of the pathway responding to high osmolarity, which results in Hog1 translocating to the nucleus activating transcription factors. Red indicates the MAP kinase module, green indicates the Sln1 branch, blue indicates the Sho1 branch, and grey indicates the phosphatases that act on Hog1. (B) Layout of the membrane associated complex. This complex has adapter proteins Sho1, Cdc42 and Ste50, and scaffold proteins Pbs2, Ste11 and Hog1 (adapted from Brewster *et al.*, 2014 [15]).

In contrast to the Sln1 branch, the Sho1 branch solely relies on serine/threonine/tyrosine phosphorylation. Besides functioning as an osmosensor, it also serves as a critical MAPK signalling adaptor linking the cell wall to MAPK (Figure 1B). Sho1 recruits proteins necessary for MAPKKK Ste11 phosphorylation and activation. There are two Sho1 sub-branches that each have their own osmosensor. The two mucin-like transmembrane osmosensors are the Msb2 and Hkr1. These osmosensors can each activate Ste11 through Sho1, but have distinct pathways. The activated Msb2 interacts with Bem1, that in turn recruits Ste20 to the membrane. In contrast the Hrk2 pathway does not require Bem1. Following hyperosmotic stress Pbs2 is recruited to the membrane, carrying

along Ste11 that in turn interacts with Ste20 and Cla4 [16]. Phosphorylation of Ste11 by either Ste20 or Cla4, activate Ste11, which together with Ssk2/Ssk22 phosphorylate the MAPKK Pbs2. Pbs2 in turn phosphorylates and activates the MAP kinase of the pathway, Hog1 (Figure 2). Interestingly, even though both of these osmoadaptation branches ultimately converge on Hog1, cells can still survive high osmotic shock upon its deletion [17]. This suggests that there may be redundancies in yeast osmoadaptation process.

1.3 Synthesis of glycerol during osmoadaptation

High extracellular osmolarity affects the expression of hundreds of genes [15]. This begins with phosphorylated Hog1 translocating and accumulating in the nucleus. Some of the well-known transcription factors regulated by Hog1, in the nucleus, are Hot1, Msn1, Sko1, Msn2 and Msn4 (Msn2/4). The genes GPD1 and GPP2, which encode for enzymes involved in the glycerol biosynthesis —a hallmark of osmoadaptation— are activated by the transcription factor Hot1 [18], [19].

Recent genetic profiling has revealed an overlap of hundreds of genes that are upregulated in response to osmotic shock and other stresses [20]. These common genes, which are involved in various kinds of stress responses are called stress responsive element (STRE) [21]. Similar to osmoadaptive response, the activation of STRE is triggered by two homologous zinc finger activators, Msn2/4. These activators bind to a conserved STRE, at 5′-CCCCT-3′, located in the promoters of these genes [22]. Under homeostasis conditions the activators Msn2/4 are mostly localized in the cytosol. In addition to the master regulator Hog1, an AGC kinase Sch9 is reported to also regulate Msn2/4 [23]. When cells undergo a hot/cold stress or osmotic stress, hyperphosphorylated Msn2/4 translocates to the nucleus, in a process controlled by the cyclic AMP (cAMP)-dependent protein kinase A (PKA) [24]. Interestingly, a phosphoproteome study on budding yeast investigated the regulated phosphopeptides as cells were exposed to hot/cold stress. This study concluded the involvement of the target of rapamycin complex1 (TORC1), and its substrate Sch9 and thereby PKA in the upregulation of STRE genes (Kanshin *et al.,* 2015, [25]).

For cells to survive high osmolarity, another imperative feature besides the actual

glycerol synthesis, is to keep synthesized glycerol within the cell. The accumulation of glycerol is ensured by the closure of the transmembrane aquaglyceroporin Fps1 [15]. The mechanism of Fps1 function was described in detail in Kanshin & Bergeron-Sandoval *et al.,* 2015 [26]. In summary, Hog1 phosphorylation of the regulator glycerol channel 1 and 2 (Rgc1 and Rgc2) causes their release from Fps1, which leads to the closure of Fps1 [27]. Despite this, Hog1 is not an essential gene. Remarkably *HOG1Δ* cells are able to proliferate when exposed to 0.2M NaCl, just like their WT counterpart [28][29][30]. At high osmolarity, 0.4M NaCl, *HOG1Δ* cells stop proliferating, but do not die [12][30][29]. It is not fully clear how cells are able to tolerate high osmolarity stress. However, a series of recent studies have indicated an involvement of target of rapamycin (TOR) via Ypk1 in the regulation of glycerol synthesis and Fps1 activity. More specifically, due to high osmolarity, inactivation of TORC2-dependent effector kinase Ypk1 leads to de-phosphorylation of Gpd1. This accelerates cell recovery through increased glycerol production [31][32]. Intriguingly, Fps1 is also an authentic substrate of TORC2-Ypk1. It was shown that the TORC2-Ypk1 complex regulates the extent to which the Fps1 channel lets out excess glycerol, which is a vital part of osmoadaptation [33]. These data make TOR a central player in cellular osmoadaptation.

1.4 Osmotic shock causes Hog1 to translocate to nucleus leading to a temporary cell cycle arrest

How cells perturb their growth machinery in order to survive high osmolarity is an active field of study. Cellular response to osmotic shock starts as soon as available water (opposed to bound water) in cytosol is lost to the extracellular space. Hog1 translocates to the nucleus within 1-5 minutes and remains in the nucleus over a period of 20 minutes (Figure 2B). After 72 minutes of exposure to high osmolarity, Hog1 totally returns back to the nucleus and cycle resumes. The new cellular state allows cells to proceed with cell cycle even under the osmotic pressure, Figure 2A [34]. With regard to how cells adapt to osmotic shock depends on which phase of the cell cycle a cell is as it is exposed to high osmolarity. The cell cycle can be divided in four phases in the following order: G1, S, G2 and M.

6
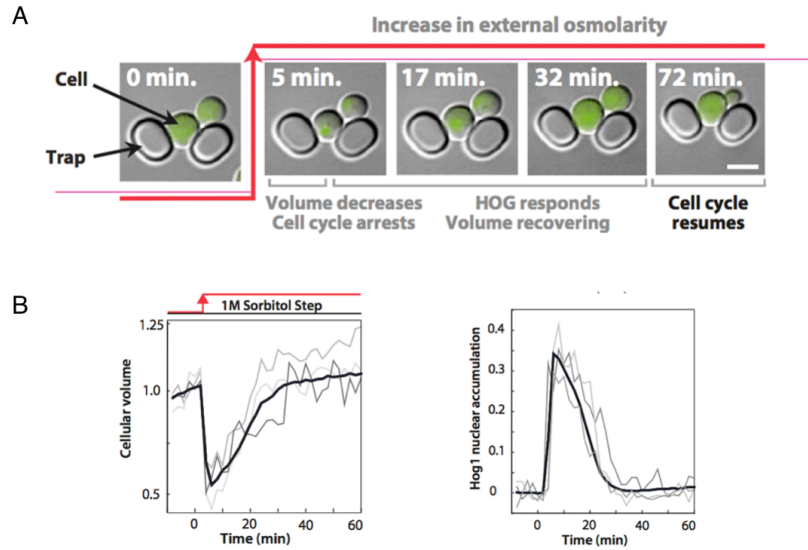
Figure 2: High osmolarity affects cell cycle, cell size and Hog1 nuclear localization.
(A) Cells that are trapped in a microfluidic device. Osmotic shock is applied using a step function, using 1M sorbitol. Hyperosmotic shock results in shrinkage of cellular volume, translocation of Hog1 to the nucleus, and cells arrest is seen almost instantly. (B) The reduction in volume and Hog1 to translocation occurs almost simultaneously. Recovery of the cell volume and the amount of nuclear Hog1 relocating to the cytosol completes after 30 minutes. After 72 minutes cells then resume cell cycle. Cell number: n=356, the three single-cell traces are selected randomly. (This figure was adapted from Granados *et al.,* 2017 [34])

Different pathways are likely to be involved for temporarily arresting the cell cycle. For example, Hog1, that is localized in the nucleus, probably will have different substrates that in turn prevent cells from passing the G1/S checkpoint, compared to the G2/M checkpoint or spindle checkpoint [10]. Thus, cells will likely have heterogeneous responses to high osmolarity, which is to some extent contrary to the finding of STRE genes previously covered.

The G1 phase of the yeast cell cycle is the phase between the end of the previous mitosis until the beginning of DNA synthesis. This phase is the longest part of the cell cycle in budding yeast; it is approximately 2.5 times longer than the rest of the cell cycle [35]. Between the G1 and the S phase exists a checkpoint that ensures a cell-size threshold is exceeded, and furthermore, cells are able to assess whether environmental conditions are suitable to proceed to the S phase [36]. It is already reported that osmotic stress delays G1 phase and thus cell cycle entry [37], in a Hog1 dependent manner, but the molecular

mechanisms of how this is achieved are not fully understood.

The G1/S checkpoint hinges on regulation of two heterodimeric transcription factors: SCB-binding factor (SBF) and MCB-binding factor (MBF) [38][39]. SBF regulates the genes that code for G1 specific proteins. SBFs DNA binding component is Swi4 [40]. Due to the binding of a transcriptional repressor Whi5 to SBF, the upregulation of G1 specific genes are inhibited, until the G1/S checkpoint [41]. The release of Whi5 occurs upon its phosphorylation by a complex consisting of a kinase Cdc28 and its activating cyclin protein Cln3 [42]. However, it should be noted that this model has known redundancies [43][44][45][46]. In section 3.4, some of the phosphosites that could be implicated in this process are studied and explained.

1.5 Functional and promiscuous phosphorylation

With the advent of sensitive mass spectrometry (MS) and affinity media, for phosphopeptide enrichment, proteome-wide phosphoproteomic studies were suddenly possible requiring only a very small sample size. This was a significant breakthrough as phosphorylation is one of the most prevalent post-translational modifications. Many biological functions depend on phosphorylation and de-phosphorylation, which ensure cell homeostasis and stress adaptation. Phosphorylation is a covalent reaction by which a kinase enzyme catalyzes and transfers a phosphate group from adenosine triphosphate (ATP) (or guanosine triphosphate) to usually serine (S), threonine (T) or tyrosine (Y), or less typically histidine (H), arginine (R) and lysine (K), like in the two-component system seen in the Sln1 branch part of the cellular osmosensor (Section 1.2) [47]. Dephosphorylation is the opposite, by which a phosphatase catalyzes the transfer of a phosphate group away from an amino acid residue to a water molecule. Mass spectrometry studies have raised the possibility that most protein phosphorylations are inconsequential in terms beneficial phenotypes [48][49]. However, it should be noted that these phosphorylations can pick up significance with other additional mutations that can occur over an evolutionary significant time scale [50]. In addition, with the current state of the art technology, it is still too early to state that every protein phosphorylations in S. Cerevisiae has been discovered. Mass spectral data is only capable of showing protein phosphorylation. It does not indicate any information whether a site on a protein can not be phosphorylated.

Phosphorylation in yeast and humans happens on a massive scale regardless of whether it is functional or not. The total number of enzymes that have a kinase or a phosphatase function, is 644 in humans [51] and 159 in budding yeast (yeastkinome.org). If we assume that each enzyme has a dozen interaction partners, it becomes evident that this would result in a very complex network. In addition, when off target phosphorylation (promiscuous phosphorylation) are taken into account, the network becomes even more complex [52][50], so much so that the kinase-phosphatase (KP) networks could in fact be irreducibly complex [53][54]. A recent study has estimated that KP's could phosphorylate/dephosphorylate as much as 60% of all budding yeast proteins [55].

To address the complex nature of kinase and phosphatase network and to give a rational insight, some studies have opted for *in silico* analysis. These studies use elegant assumptions and criteria that in turn systematically attempt to capture functional interactions from those that are not. Some of these criteria are the following: functional phosphosites occur in less abundant proteins, functional phosphosites are sequence-wise more conserved, functional phosphosites have higher phosphorylation stoichiometry, and phosphosites with known function evolve slower [52][49][56][57][58][59]. However, these criteria are not perfect and their validity will be more clear over time [60]. In parallel to this, with already *gained in vivo* knowledge, significant effort has been made to map the kinase-phosphatase network [53][61][62][63]. These *in silico* analyses, and *in vivo* studies, together with data from high throughput mass spectral analysis will over time give a better picture to the already well-studied kinase and phosphatase networks.

1.6 Hierarchical structure of kinase and phosphatase networks

Networks can relay complex interaction information visually by nodes and edges that connect them. Some prominent examples of networks are the World Wide Web, citation relationships and biological processes. Networks are made of nodes and edges. Nodes can be proteins in the scope of our interest, and edges reflect the relation between the proteins. A network can be divided into two depending on the properties of its edges. In a directed network, there is directionality; like an enzyme and its substrate, where as an undirected network has no directionality information. When a directed network is made up of edges that are asymmetrical, it consequently generates a hierarchical network structure.

This in turn can result in network layers such as top, core and bottom, depending on the nature of the network [64].

One recent hierarchical network that illustrates the KP network was recently curated by a former colleague, Abd-Rabbo & Michnick, 2017 [65]. The topological network structure seems to resemble a bow-tie shape, and is made out of 3 layers (bottom, core and top), reflecting different biological properties (Figure 3). To associate biological roles with these three layers a Gene Ontology enrichment and depletion analysis was utilized, Abd-Rabbo & Michnick, 2017 [65]. The postulated biological functions associated with each layer are the following. The top layer is enriched with proteins with high abundance, and low noise (a concept defined in Newman *et al.*, 2006 [66] that uses the coefficient of variation (CV) of protein abundance (the ratio between the protein standard deviation to its mean abundance)), which are thought to play a role with the fidelity of the biological signals. The core is enriched with proteins that are associated with scaffolds, take part in cell cycle and organization, and are localized to a sub-cellular compartment such as the bud neck. The nodes that make up this layer are more connected than the other two layers, and it forms a bottleneck within a bow-tie structure, which in turn suggests a decision-making quality and signal integrity within the core layer. And lastly, the bottom layer is enriched with few GO terms which suggests that these proteins are less specialized compared to those in the other layer.
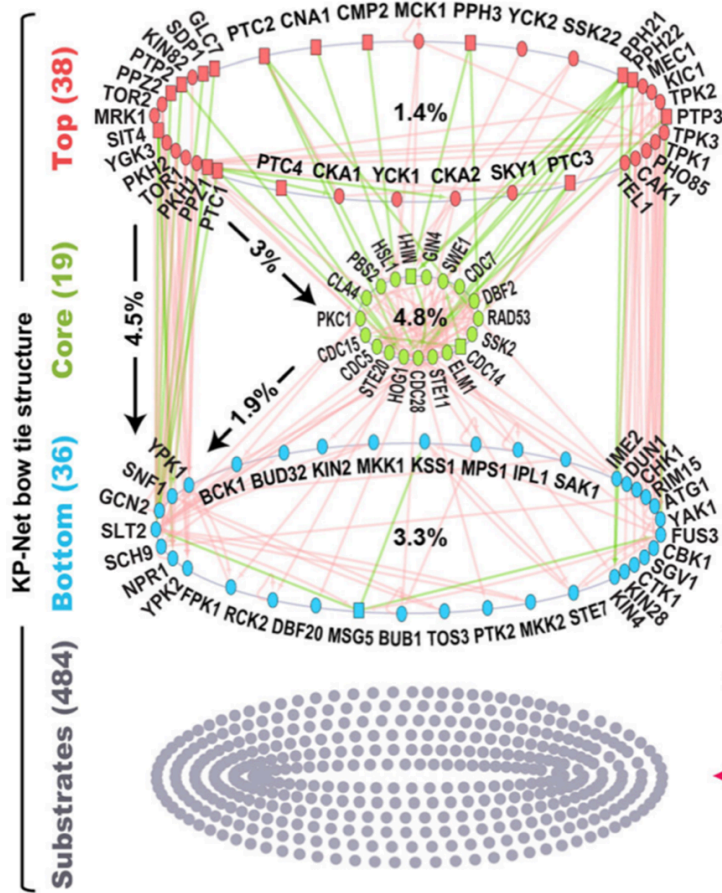
Figure 3: The architecture of the kinase and phosphatase network.
The general architecture of 101 of kinase and 31 phosphatase (covering 77%) can be evaluated as a bow-tie. The core level is classified as a strongly connected component, later the top level was formed as the layer that regulates the core layer, and lastly, the bottom layer was formed and is the layer that the top and core layer regulates. The direct interaction number that are not KPs are 484, which are mostly KP substrates (adapted from Abd-Rabbo & Michnick , 2017 [65]).

This network reflects our current knowledge of what we know about kinases and phosphatase, but it is not perfect. This is because our knowledge is not complete: phosphatases are not as well studied as kinases, nonspecific phosphorylation of kinases cause false positive results, and a significant portion of our existing interaction network comes from protein-protein interactions, genes deletion, and genetic interaction assays, which in turn create fundamental problems such as causality as directionality between nodes are not always clear [62][54]. Despite this, these networks are also a valuable source for connecting ideas and biological interactions.

1.7. Investigating kinase-phosphatase networks using mass spectrometry

1.7.1 Mass spectroscopy and SILAC

Mass spectroscopy-based proteomics is an indispensable tool of choice when it comes to quantifying and identifying large-scale protein phosphorylation [67][68]. There are 3 main components to a mass spectroscope (MS): an ionizer, an analyzer to separate fragmented peptides, and a detector that measures these peptides that have a certain mass-to-charge (m/z) value. The peptides are created by digesting the entire protein soup using an enzyme called trypsin. This protease cleaves proteins by hydrolyzing peptide bonds at sites adjacent to arginine or lysine residues.

Electrospray ionization (ESI) is a technique used in mass spectrometry that produces ions for their eventual detection [68]. The ionization process occurs when macromolecules in a solution pass through a vacuum capillary. These capillaries are electrically heated and with the application of a large potential difference the sample is dispersed into fine aerosols (3-10 nm). Water-based solvent evaporates and gas-phase ions are produced. These ions are later sent into the mass analyzer with a carrier gas [69].

The ions created are then directed to the mass analyzer. To redirect and trap these charged peptides, magnetic and static fields are utilized [70]. One such devise is the Orbitrap. It has an outer and an inner barrel electrode that traps ionized peptides within a circularly confined space [71]. These ions oscillate axially depending on the peptide mass-to-charge ratio (m/z), resulting in their separation. The image current on the outer electrodes, induced by ion axial motion, is measured as a time domain transient and then fast Fourier-transformed to produce a frequency spectrum, converting analog information to digital information [72]. These frequencies are then converted to m/z spectra. This process is repeated many times until the entire sample is processed. The peptide coverage of the sample can further be enhanced by coupling a linear ion trap (LTQ) that efficiently stores a large batch of charged peptides. The stored charged peptides are then injected into Orbitrap in numerous smaller batches over time.

One other key experimental setup is a liquid chromatography (LC) [73]. This step restricts the diversity of peptides simultaneously sent to the MS. By controlling the elution step on the nano-column, it is possible to control the size and quantity of the peptides that

are sent to MS. This is because peptide affinity strength (i.e. due to hydrophobic or electrostatic interaction) is determined by the amino acids that constitute a peptide and peptide length.

Once all the sample is processed by MS the extracted m/z spectra are stored for identification. Programs such as MaxQuant create libraries specific to digestion used for the experiment. Each spectrum is then compared to expected peptides and identified. The small differences in mass between the actual measurement and expected mass are then further analyzed to determine the post-translational modification specific to each peptide. Compiling all the deduced post-translational modification specific to unique peptides enables us to understand which proteins are regulated by post-translational modifications specific to an experiment.

Differential analyses are experiments where an experimental condition is compared to a control group lacking that condition. One MS experimental technique used for differential analysis is Stable Isotope Labeling with Amino acids in Cell culture (SILAC) [74]. This is a reliable way for detecting stimuli specific post-translational protein modifications. To perform a SILAC experiment, a sample of cells is grown in a medium containing amino acids composed of natural abundant isotopes (e.g. $^{12}C/^{14}N$), and the second sample is grown in amino acids labeled with stable heavy isotopes (^{13}C and/or ^{15}N labeled arginine and/or lysine). By virtue of what is present in the culture media, cells that are lacking enzymes for the synthesis of arginine and/or lysine, will eventually incorporate amino acids with isotopes (^{13}C or ^{15}N) in all newly synthesized proteins. Thus, by associating an experimental condition to peptides with heavy isotopes it becomes possible to make differential analysis. These peptides are prepared in the following order: cell lysis, protein extraction, enzymatic digestion and phosphopeptide isolation, which are described separately in the Method Section 2.3, 2.4. 2.5, and 2.6.

1.7.2 Phospho-kinetic profiles of kinases and phosphatases in sub-minute and half-hour timescales, in response to osmotic shock

To elucidate phosphosites that are regulated over time, budding yeast was first exposed to high osmolarity using 0.4 M NaCl. Control cells were grown in light isotope, and

cells exposed to NaCl were grown using culture that had heavy isotopes of arginine and lysine. Two different timescales were used: 60-second exposure to osmotic shock (same data as in Kanshin & Bergeron-Sandoval , *et al.,* 2015 [26]), and 33-minute exposure to osmotic shock. In short, these will be referred to as the 60-second response study and 33-minute response study. As a result of these studies both regulated (phosphorylated) and non-regulated (not phosphorylated) phosphopeptides were measured. The general aim was to first distinguish between regulated and unregulated phosphopeptides, and then extract biological significances.

1.8 Research project

My memoire recapitulates some of the essential results generated in the paper, "A Cell-Signalling Network Temporally Resolves Specific versus Promiscuous Phosphorylation," Kanshin & Bergeron-Sandoval *et al.,* 2015 [26], where I contributed to the analysis of the data and became a second author. The paper investigates budding yeast proteins with dynamic phosphosites (regulated proteins) in response to high osmolarity (0.4 M NaCl), over a time period of 0-60 seconds. The second part includes the dynamic phosphosites extracted from 0-33 minute data, which was not included in this paper, nor analyzed.

1.8.1 Problem and hypothesis

Finding functional kinases and phosphatases that play an active role in osmoadaptation in *S. cerevisiae* is still an ongoing research field. Much is known in terms of the proteins that take a part in the sensing of extracellular osmolarity, and how the HOG-MAPK pathway relays these signals downstream for the osmoadaptation. However, until recently (Kanshin & Bergeron-Sandoval *et la.,* 2015 [26]) proteome-wide kinetics of phosphopeptides during osmoadaptation was not studied. The was because the advent of sensitive mass spectrometry (MS) and affinity media for phosphopeptide enrichment was only possible with leaps made in MS during late 1980s and the discovery of SILAC technique in the early 2000s [69][74]. The phosphorylation dynamics could fill some of the gaps present in our understating of how signalling works during osmoadaptation.

Early on in the research project, it was hypothesized that functional interactions

between KPs and their substrates were postulated to be more optimized when compared with their off-target (promiscuous) substrates. This also meant that the protein-protein interaction network responding specifically to the stimuli would also be more enriched when compared to their off-target substrates. This supposition hinges on two ideas. First, optimized interactions occur sooner and faster when compared to other non-functional interactions. Second, the protein-protein interaction network that responds to a particular stimuli becomes more complex as time progresses. Thus, measuring phosphodynamics at sub-minute high temporal resolution could provide an accurate, stimulus-specific measurement of phosphoproteome changes, and lead to the discovery of more functional phosphosites.

In this memoire, it was hypothesized that cells undergoing osmotic shock —that have not crossed the G1/S checkpoint— would have an advantage over those that have crossed into S phase. This is because the energy needed for DNA replication is quickly reinvested into biological processes that would prepare the cell against stress, which is caused by non-ideal environmental conditions, such as abrupt water loss due to high osmolarity. However, the osmoadaptation process of budding yeast is far longer than 1 minute. The initial phase of the osmoadaptation takes about 30 minutes. During this initial phase cell volume is readjusted with the newly synthesized glycerol, and Hog1 over time localizes back to the cytosol. The osmoadaptation process completes as cell cycle progression restarts, and this happens only after ~70 minutes after the initial osmotic shock (Figure 2). Thus, a larger timescale was required to observe the dynamic phosphosites involved in the yeast osmoadaptation process. Fortunately, our lab had made another set of experiments on budding yeast, looking into the osmoadaptation over a longer time period of 0-33 minutes. This was never used, probably due to concerns over causality between stimulus and cellular response, and perhaps concerns over off-target MS readings masking functional interactions. In general, data reproducibility in MS studies has traditionally been a struggle. In Kanshin & Bergeron-Sandoval *et al.,* 2015 [26], a preliminary analysis with less temporal resolution was made that increased the confidence in the sub-minute MS data. In my memoire, it was possible to compare and use the sub-minute data together with the 33-minute MS dataset, which was previously not used. Looking at initial results in the 33-minute data, it was re-hypothesized that it was possible that functional phosphosites were not masked by off-target phosphorylation. Consequently, it would mean that the

interaction network was not as complicated as initially thought.

Moreover, it is known that Hog1 is not an essential gene. Yeast cells are able to survive osmotic shock without Hog1. Therefore, it is supposed that other pathways are still in play during the osmoadaptation process and we may be able to answer how these other pathways work together with MAPK-Hog1 signaling. These other rescuing pathways could be part of a bigger stress response mechanism that helps cells cope in non-ideal external conditions. By making use of the MS data elucidating phosphodynamics on both timescales and combining these results with readily available protein-protein interaction datasets could help elucidate other processes that occur in osmoadaptation.

1.8.2 Research objectives

Studying the structure and the dynamic behavior of networks underlying biological processes in response to high osmolarity can possibly be achieved by looking at initial response and later response. Thus, some of the goals are listed below:

I. Describe the experiment pipeline and how enriched peptides were obtained from the SILAC-based MS analysis. Introduce the output generated by the MS analysis and introduce the criteria used for identifying high-confidence regulated phosphosites.

II. Clearly display the discovered regulated phosphosites on both osmosensors branches, Sln1 and Sho1, and the subsequent sequential kinases: a MAPK Kinase Kinase (MAPKKK), MAPK Kinase (MAPKK) and MAPK, which constitute the classic osmoadaptation pathway.

III. Investigate other pathways, besides MAPK-Hog1, that may be involved in the osmoadaptation process. Determine the possible pathways that help yeast cells to survive during osmotic shock? Determine if there are other adaptation processes that exhibit similarities with the osmoadaptive process and indicate the overlapping dynamic phosphosites.

IV. Cells exposed to high osmolarity require time to adjust. Until they are able to adjust, the cell cycle is temporarily stopped. This process probably occurs differently depending on which phase of the cell cycle a cell is in. However, G1/S checkpoint was particularly

investigated because every cell that will undergo a cell division will likely to remain at this checkpoint for a significant amount of time. Determine the possible phosphosites that likely may be involved in cell cycle, and even significant in terms of how cells commit to cell division.

V. Determine an empirical formula for all high confidence phosphorylation kinetics for peptides (static and dynamic) during the sub-minute and the half-hour timescales of the osmoadaptive process. Determine regulated phosphopeptides and global trends using clustering.

VI. Retrieve the regulated KPs during osmoadaptation process during the sub-minute and half-hour timescales. Make an interaction network using only KP's and check whether there are overlaps between the networks between responses over these different timescales. Determine whether protein abundance is a factor in the kinetics of the phosphopeptide. Also project these regulated KPs onto the bow-tie hierarchical network (Abd-Rabbo & Michnick, 2017 [65]), to further gain an understanding in biological functions.

VII. Find the regulated genes and/or the specific phosphosites that have a kinetic profile within the sub-minute and half-hour timescales of the osmoadaptive process. Perform a Gene Ontology analysis on these common genes and update the extensive interaction network generated in Kanshin & Bergeron-Sandoval et al., 2015 [26].

VIII. Recapitulate some of the data in Kanshin & Bergeron-Sandoval et al., 2015 [26], linking phospho-null mutants to the reduced cellular fitness, which in turn underlines the biological significance of the discovered dynamic phosphosites.

1.9 Contribution of the Author

The mass spectral data for the sub-minute and half-hour timescales was produced by Evgeny Kanshin. I, together with Louis-Philippe Bergeron-Sandoval contributed to the phosphoproteomic analysis for the sub-minute timescale, which was used in Kanshin & Bergeron-Sandoval et al., 2015 [26]. All in vivo work was made by Louis-Philippe Bergeron-Sandoval. I created the two empirical models that was used for describing the entire MS data, both for the sub-minute and half-hour timescales. I, together with Louis-Philippe Bergeron-Sandoval determined the regulated peptides for the sub-minute timescale, which was published in the paper [26]. I determined the regulated phosphopeptides for the half-hour timescale. I made all the bioinformatic analysis comparing these regulated phosphopeptides between the sub-minute and the half-hour timescales.

2. Methods

2.1 Cell Culture

Quantitative SILAC mass spectroscopy was performed on the yeast strain S288c. This strain lacks genes coding for argininosuccinate lyase (*ARG4*) and saccharopine dehydrogenase (*LYS1*), S288c LYS1Δ::kanMX; ARG4Δ::kanMX, obtained from Ole Jensen, University of Southern Denmark. Control cells were grown in Synthetic Dextrose (SD) medium with added light Lysine and Arginine (^{12}C-, ^{14}N-). Cells that were exposed to the stimuli were grown in SD medium with added heavy Lysine and Arginine (^{13}C-, ^{15}N-). Isotopes were purchased from Cambridge Isotope Laboratories. Cells were inoculated in 50 ml SD medium that contains 2% glucose, 0.17% yeast nitrogen base without amino acids, 0.5% ammonium sulphate and required amino acids. The 50 ml culture would further be split into two 25 ml cultures. Light isotopes were added to one and the heavy isotopes were added to the other, with the concentration of 20 mg/L for arginine, and 30 mg/L for lysine. After incubating cells for about 7 to 9 doubling times, L-proline (20 mg/L) was added to the cultures to prevent cells converting arginine to proline. Cells were then grown until late-exponential phase, OD_{600} ~0.8-1, and at this stage the cells had incorporated 100% of the isotope labeled arginine and lysine.

2.2 Applying osmotic stress

Cells incubated with heavy isotopes were grown until late exponential stage (OD_{600} ~0.8-1) and then treated with NaCl, at a final concentration of 0.4M (using a stock SD medium that contains 4M NaCl, at 30 degrees Celsius). Cells incubated with light isotopes were also grown until late exponential stage and treated with 2.5 ml SD medium without NaCl (at 30 degrees) that would serve as a control. The number of samples collected for cells exposed to 0.4M NaCl over 0-60 second and 0-33 minute timescales were 13 and 23 respectively. Samples, specific to these timescales, were collected over equal time intervals. A maximum time resolution of 5 seconds was needed during the 0-60 second timescale. In order to achieve this kind of time resolution cells growing in light and heavy

isotopes were quickly pooled together (into 50 ml culture) and frozen in a 500 ml liquid nitrogen. All these samples were then stored at -80°C.

2.3 Cell lysis

Freezer mill apparatus (Biospec) was used for lysing cells under liquid nitrogen. Grinding efficiency was checked by utilization of microscopy. For the 50 ml culture (OD_{600} 0.8-1), 32 cycles with each cycle containing 2 minute maximum intensity grinding and 2 minute cool down ensured a 90% and above lysis efficiency. Culture powder was stored at -80°C.

2.4 Protein extraction

TCA was used to concentrate and purify proteins from other cell debris. An equal volume of 30% TCA solution was incubated with grounded culture powder for 2 hours. These samples were then centrifuged at 20,000x g for 20minutes, at 4°C. Protein pellets were washed twice using 10 ml cold 10% TCA, discarding supernatant each time. Final wash of the pellet was made using cold acetone, and protein pellets were then resolubilized in 8M urea buffer (8 M urea, 100 mM Tris pH8.0, supplemented with HALT phosphatase inhibitor cocktail by Pierce). Solubilized proteins are suspended within the supernatant, and were further purified by centrifugation at 40,000g for 10 minute. Bicinchoninic acid assay (BCA) from Thermo Fisher Scientific is was used to measure protein concentration.

2.5 Enzymatic digestion

Protein disulfide bridges were broken by incubating samples with dithiothreitol at a concentration of 5 mM for 30 minutes at 56 degrees Celsius. Samples were allowed to cool down at room temperature. Reduced cysteines were alkylated by treating the sample with 15 mM iodoacetamide for 30 minutes, in a light sealed container at room temperature. Alkylation was stopped using 5mM dithiothreitol for 15 minutes. Samples are diluted 6 times using dilution buffer (20 mM TRIS pH 8, 1mM CaCl2), and then trypsin was added at a mass ratio of 1:50 (trypsin:substrate). Trypsin digest was done overnight at 37°C and was

stopped by adding formic acid at a 1% final concentration. The suspension was purified at 20,000g for 10 minutes, and desalted using the Oasis HLB cartridges. Peptide elutes were flash frozen using liquid nitrogen, and lyophilized using SpeedVac before being stored at -80°C.

2.6 Phosphopeptide isolation

The enrichment of phosphopeptides was done using custom made pipet tips. The volume of the pipet tip was 200 μL and it used SDB-XC membrane-TiO2 beads as previously described [75]. SDB-XC material is hydrophobic and allows phosphopeptide enrichment and desalting. The enrichment protocol consisted of loading, washing and elution [76][77]. These columns were first equilibrated with the loading buffer (250 mM lactic acid in 70% acetonitrile (ACN) 3% trifluoroacetic acid (TFA)), and then 100 μL of loading buffer was used for solubilizing peptides, which was then applied to the column. Each column was washed with 100 μL of loading buffer followed by 2 x 100 μl of 125mM asparagine and glutamine in 70% ACN 3% TFA and 100 μl of 70% ACN 3% TFA. Subsequent washing with 50 μl of 1% FA was used to equilibrate SDB-XC frit material. Phosphopeptides were eluted from TiO2 with 2 x 50 μL portions of 500 mM Na2HPO4 pH 7 and retained on SDB-XC. To desalt, 50 μl of 1% formic acid was used. And the final elution from the SDB-XC was made with 50 μl of 50% ACN and 0.5% formic acid. The eluted volume was then dried with SpeedVac and stored in -80°C.

2.7 Off-line fractionation of phosphopeptides

Before MS analysis, SCX chromatography fractionation was utilized to increase the coverage range of phosphopeptides. Peptides were solubilized in 100 μl using loading buffer (0.2% formic acid and 15% ACN) and loaded onto StageTips containing 6mg of Poly-sulfoethyl-A SCX phase. These columns were then washed once using 50 μl of loading buffer, and then eluted in 100 μl, using a NaCl concentration ramp in the following order: 40, 70, 100, 150 and 500 mM NaCl in loading buffer. Flow-through and salt fractions were then dried using SpeedVac and re-suspended in 15 μl of 4% formic acid, later to be analyzed by nanoLC-MS/MS.

2.8 NanoLC-MS/MS

The enriched peptides were analyzed with MS (m/z ratios for the peptides) and MS/MS (selected m/z ratios for further spectral analysis), using online reverse phase chromatography (HPLC) followed by an electrospray ionization (ESI). The HPLC system (Eksigent, Thermo Fisher Scientific) used a reverse-phase pre-column, where peptides were concentrated in 5mm long traps (300 μl inner diameter), and were separated along 18mm fused silica capillary analytical columns (150 μl inner diameter). Each column would pack 3 μm 200Å Magic AQ c18 non-polar reverse-phase material. LC separations were performed at a flow rate of 0.6 μl/min using a linear gradient of 5–40% aqueous ACN (0.2% FA) in 100 min. After elution, columns were washed with 80% ACN (0.2% FA) and re-equilibrated with 5% ACN (0.2% FA). The HPLC solvents used were 0.2% formic acid (Solvent A), ACN and 0.2% formic acid. Total run time was 125min. This included the sample loading and column conditioning. MS spectra were acquired with a resolution of 240,000 using a lock mass (m/z: 445.120025) followed by up to 12 MS/MS data-dependent scans on the most intense ions using collision induced dissociation. AGC target values for MS and MS/MS scans were set to 1e6 (max fill time 500 ms) and 1e5 (max fill time 50 ms), respectively. The precursor isolation window was set to m/z 2 with a CID-normalized collision energy of 35. The dynamic exclusion window was set to 60s.

2.9 MS Data processing and analysis

The acquired MS data were analyzed using MaxQuant software version 1.3.0.3 [78][79]. A total of 5,904 peptides for the 60s experiment, and 3,564 peptides for the 33min experiment were identified using the SGD database. Common laboratory contaminants were included in MaxQuant, together with their reversed sequence versions (248 entries). The enzyme specificity was set to trypsin with a maximum number of missed cleavages set to 2. The precursor mass tolerance was set to 20 ppm for the first search (used for nonlinear mass re-calibration [79], and then to 6 ppm for the main search. Phosphorylations on serine, threonine and tyrosine residues were examined (variable modification); carbamidomethylation of cysteines were considered as a fixed modification. Peptide site

22

identification false discovery rate (FDR) was set to 1%, the minimum peptide length was set to 6, and the "peptide requantification" function was enabled. To correlate identification and quantitation results across different runs, the option match between runs (1-min time tolerance) was enabled. MaxQuant parameters can be found in Kanshin & Bergeron-Sandoval *et al.*, 2015 [26], having file names parameters.txt and experimentDesign.txt.

Additional conditions were implemented to raise the quality of the data extracted. In addition to the FDR, there were three more filters applied to gain high confidence phosphopeptide time profiles. First, every time profile needed to have at least 10 data points (out of 13 discreet time points that amount to 1 min) for 60s data and 20 data points (out of 23 discreet time points that amount to 33 min) for 33min data. Second, each identified phosphosite had to have a confidence probability higher then >0.75. This probability means that if there were two phosphosites on a single peptide the probability of estimating the actual site correctly is at least 0.75 (palindrome-like sites decrease this probability). Third, every time profile unique to a peptide would need to have at least 3 significant fold change values. When these conditions were applied a total of 5,904 high confidence temporal profiles (for the 60 second experiment), and 3,564 high confidence temporal profiles (for the 33 minute experiment) were extracted.

2.10 Accessing significance of phosphosites

A standard way of identifying regulated peptides is by using FC values. A FC value of 2 corresponds to a two fold up-regulation, and its converse would indicate a down-regulation of 2 folds. However, the majority of extracted high confidence temporal profiles do not have a FC value of 2 or 1/2. To distinguish the modified peptides (dynamic profiles) from those that are not modified (static profiles), a statistical test was applied in MaxQuant using fold change (FC) values. The test uses a true negative set from all the peptides that could not be modified (Kanshin & Bergeron-Sandoval *et al.* 2015 [26]), and the test used significance of p-value<0.05 (with correction for multiple hypothesis testing).

For the 60s experiment, using the statistical test provided 638 dynamic profiles. The main drawback of using such a method was that it eliminated phosphosites with low FC ratios. Therefore, to increase this number, a complimentary analysis was performed that would take in account the discrete change in FC ratio. Every kinetic profile was transformed

into a signature. Each signature would be a series of positive change (+) and negative change (-), i.e a sequence {2,10,1,5} would be transformed to {+, -, +}. This method (up-down analysis) has been used in genetic expression screens [80][81], and hinges on the assumption that transformed random signatures must fluctuate randomly showing no correlation.

The probability P (σ) that N + 1 random data points have a signature σ is

$$P(\sigma) = C(\sigma)/(N + 1)!. \qquad (1)$$

For example, the frequency C(σ) takes its minimum value when the data are monotonically increasing {+,+,+…} that indicate up regulation or decreasing {-,-,-…} that indicate down regulation.

The probability that all of the M random signatures have frequency greater than C(σ) is

$$A(\sigma, M) = F(\sigma)^M. \qquad (2)$$

The cutoff applied to this analysis was A(σ, M)=0.9. The quantity 1/[1 – A(σ, M)] is the number of times we would need to repeat a random experiment in order to find a kinetic profile with signature σ. In addition to the data filtered with previously defined filters, using the up-down analysis added an addition of 116 more profiles. The total dynamic phosphopeptides increased to 737.

For the selection of the dynamic sites a simpler method was employed on the 33-minute experiment. FC values were normalized, and the selection criteria utilized both R^2 values and FC values. Equation 4 (Section 2.11) was used for the fitting of the high-confidence temporal peptide profiles. This equation, within the 0-33 minute bound time interval, cannot exhibit rapid fluctuations. A higher R^2 value would be used for temporal profiles with smaller FC value, and the converse is applied for temporal profiles larger FC value. The exact criteria are as follows: R^2>0.6 cutoff is satisfied for profiles that have at least one log2(FC)>2, R^2>0.7 cutoff is applied for 2≥ log2(FC)>1, R^2>0.75 cutoff is applied for 1≥ log2(FC)>0.6, R^2>085 cutoff is applied for 0.6≥ log2(FC)>0.20. The negative values were used for the down-regulation. Using this method, a total of 917 dynamic high-

confidence profiles were extracted from the 33-minute dataset. This method was also applied to the 60s experiment (more than 85% of the dynamic profiles were extracted), but it was not used for the sake of accurately referencing the Kanshin & Bergeron-Sandoval *et al.* 2015 [26]. The high-confidence peptides 60-second data can be found in Table 1, and high confidence peptides 33-minute data can be found in Table 2.

2.11 Fitting of dynamic profiles

Using a custom made MATLAB program, all kinetic profiles in the 60s experiment were unified by expressing the entire data set with a single equation:

$$FC(t)=(1-c/(exp((t-d)/a)+1)) +b, \qquad (3)$$

where a, b, c and d were calculated using a non-linear least square regression model. All the kinetic profiles could be represented using only these four parameters. Because optimization problems do not always necessarily converge to the global minima it was important to supply the regression model with a start value (a=0.219 b=0.308 c=0.711 and d=0.571), a lower limit (a=1,b=-1000,c=-1000, and d=-300) and finally an upper limit (a=600, b=1000,c=1000 and d=300).

However, this empirical formula did not fit well for profiles from 0-33 minute data; the regulation pattern observed was more complex. As a result, equation 3 was modified. The equation that worked well for all traces was the following:

$$FC(t)=(1-c/(exp((t-d)/a)+1)) +b + e/exp(((log(x)-f)/g)\text{^}2),(4)$$

where the new term is highlighted. To determine the values for the parameters used in the equation the same non-linear least square regression model was used. The following start values were entered: a=0.219 b=0 c=0.711, d=0.571, e=0.043, f=10, g=100. The lower limit for these parameters were the following: a=1 b=-10 c=-1000, d=-300, e=-10, f=0, g=-100. The upper limit for these parameters were the following: a=600 b=10 c=1000, d=300, e=10, f=100, g=100.

25

Furthermore, because the empirical formula gave only 3 kinds of traces for the 60s experiment (linear, sigmoid and exponential) we further extracted maximum change, FCt_{max}, by taking the derivative (dFC/dt) and the time at which the maximum change occurred (t_{max}). All these data are listed in Table 1.

2.12 Clustering the kinetic profiles of 60s and 33min data, GO and PPI network analysis

Kinetic profiles were all clustered using "soft" clustering as opposed to "hard" clustering methods [82]. One significant advantage of a soft cluster over hard clustering is that it can filter out random data. A fuzzy C-means algorithm [83] was implemented using the Mfuzz package [84], in an R environment (http://www.r-project.org). For this clustering to work, a fuzzifier parameter and the number of clusters must be manually selected and entered beforehand. Using the mestimate function, the fuzzier parameter used for this analysis was calculated to be 1.242. To find the minimum number of clusters that covered most of the data, a range of cluster sizes were empirically tested. For every cluster tested a minimum centroid distance was calculated (the minimum distance between two cluster centers, using c-means clustering.) [85].

Using this method, 6 clusters were chosen for the 60 s data. These 6 clusters contain 596 kinetic profiles (out of 737) belonging to 332 different proteins. Each profile would have a membership value higher than 0.5. These 596 sites would be considered regulated high-confidence phosphopeptides. The number of clusters required for the 33-minute data turned out to be higher. This was because the kinetics of the phosphorylation was more complex. The number of cluster size best fit the data was 15. Each profile would have a membership value higher than 0.7. These clusters would contain 696 (out of 917) sites belonging to 405 different proteins. Similarly, these sites were considered as regulated high confidence phosphopeptides. It should be noted that because the peptide regulation kinetics are more complex in our 33 minute study, dynamic high-confidence profiles were not limited to profiles that were clustered. Thus, the entire 917 profiles were treated as regulated peptides (Table 2).

Using these dynamic profiles two networks were created for visualizing physical interactions of KPs had among each other. Each timescale (the 60-second data and 33-minute data) had their respective physical interactions network (Biogrid) [86][87]. Results

were visualized using Cytoscape; number of interactions were represented using node size, phosphatase and kinases were represented with different colors, and interactions present in one network was reflected with thinker linking lines on the other network (33 minute KP net), Figure 14.

Similarly, for proteins that were regulated in both timescales, a protein interaction network (PPI) was created using STRING [88]. All predicted PPI were based on experimental method using a minimum confidence score of 0.9. In addition, to capture indirect protein interaction an association matrix was used, which is based on the number of links that connect two proteins [89]. This is to account for proteins that are associated within a protein complex. Interaction network was retrieved from BioGrid [86][90], Figure 17.

DAVID bioinformatics resource was used to perform gene ontology (GO) enrichment analysis [91][92]. The set selected for analysis was for the proteins that had a dynamic phosphopeptides in both studies, namely the 60 second and 33 minute data, and these were analyzed against the entire S. *cerevisiae* proteome, Figure 18.

Results

3.1 Phosphoproteomic landscape of *Saccharomyces cerevisiae* as a response to osmotic shock

The experiment workflow was designed to quantitate the phosphoproteome of yeast in response to osmotic shock. Two timescales were investigated: the early cell response was measured over the first 0-60 seconds, and the later cellular changes were measured over 0-33 minutes. Temporal resolutions for these timescales were 5-second and 1.5-minute intervals respectively. This made sample preparations step especially important since ordinary cell harvesting can take anywhere between 3 to 15 minutes depending on the washing steps and centrifugation steps. Consequently, to not skew experimental results, the sample preparation needed to not exceed 5s, especially for the early cellular response. In order to prepare samples as quickly as possible, and measure the new metabolic state of cells, a new method of protein extraction was required (Figure 4A). Therefore, in order to stop cellular metabolic activity liquid nitrogen was used. This halted protein modification and their degradation. Snap freezing was performed by submerging 50 ml cultures directly into liquid nitrogen.

To investigate the peptide regulation that occurs over the first 60 seconds of NaCl treatment, 13 frozen cell cultures were used in 13 time points, and to investigate the 0-33 minutes response 23 frozen cultures were used, for a total of 23 time points. All measurements for each time point are a separate mass spectral analysis. Osmotic shock was performed on cell cultures growing in heavy isotopic forms of arginine and lysine by adding NaCl at a final concentration of 0.4M, whereas control culture were grown in light isotropic forms of arginine and lysine. These cultures would then be pooled together just before being submerged into liquid nitrogen. These frozen cultures were then ground under liquid nitrogen, washed multiple times, purified and phosphopeptides were enriched using TiO_2 resin and then analyzed using liquid chromatography tandem-mass spectrometry, 2DLC-MS/MS. (Method Section 2.1-2.7, Figure 4A) [93][94][95].

To understand the phosphoproteomic landscape change caused by osmotic shock it

is important to define interquartile range (IQR). The overall changes in phosphoproteome in response to osmotic stress were measured by the fold change (FC) ratio of peptide abundance between the two conditions. Global differences between NaCl treated and of control cells were evaluated using Mascot Percolator, by calculating the width of the log2(FC) distribution for all phosphopeptides at a given time point (Figure 4B). The distribution width is represented as the interquartile range (IQR).
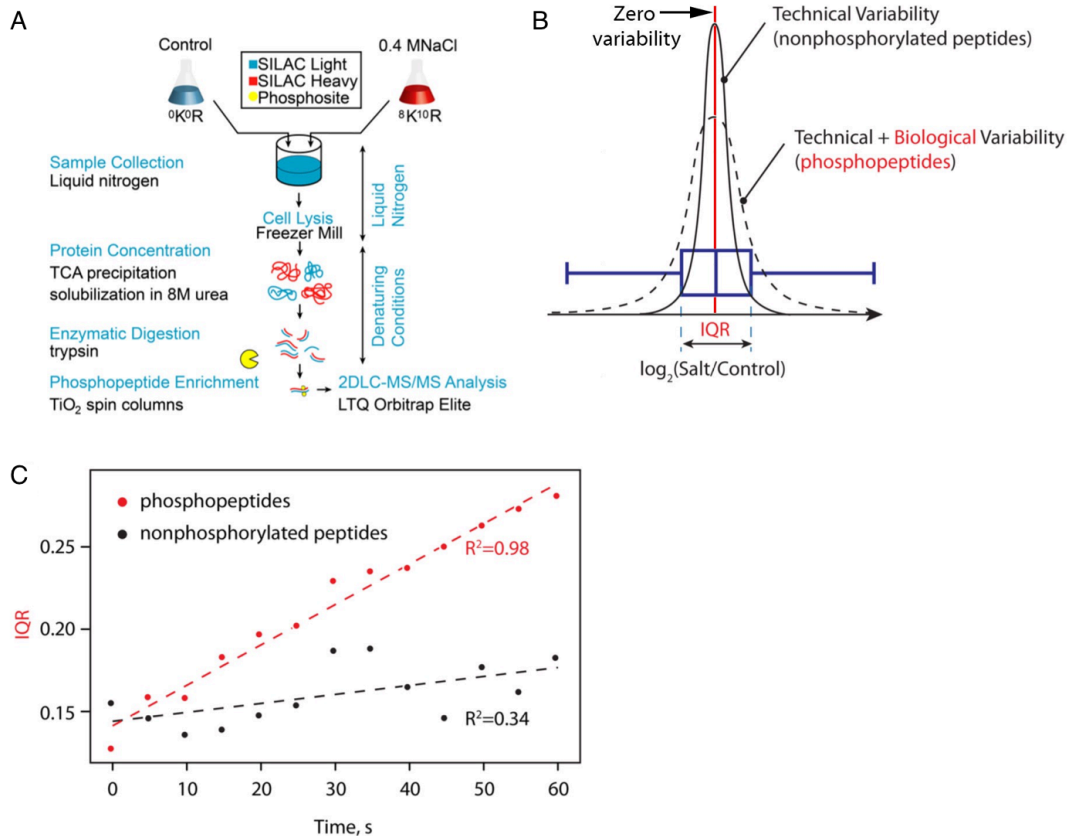
Figure 4: The summary of experimental workflow and the global effects of osmotic stress.
(A) Experimental workflow to study phosphoproteome dynamics at high temporal resolution and 33-minute timescale. Samples are collected by flash freezing yeast cultures in liquid nitrogen to prevent protein modification and degradation. (B) An increase in width of IQR distribution is usually indicative of biological variability caused by a stimulus, in this case osmotic stress. Thus, all recorded positive and negative FCs for proteins, upon osmotic stress, are represented by an IQR created in Mascot Percolator. (C) Phosphopeptides exhibited a progressive increase in IQR over time, reflecting the global effects of osmotic stress on the entire phosphoproteome.

In the case of NaCl treatment, global phosphorylation changes would cause a widening of the FC distribution. At time zero, no significant difference was observed in the IQR values for both dynamic and static temporal profiles. This changes progressively as time increases and after 15s of exposure to NaCl IQR indicates a significant change in global phosphorylation data (Figure 4C).
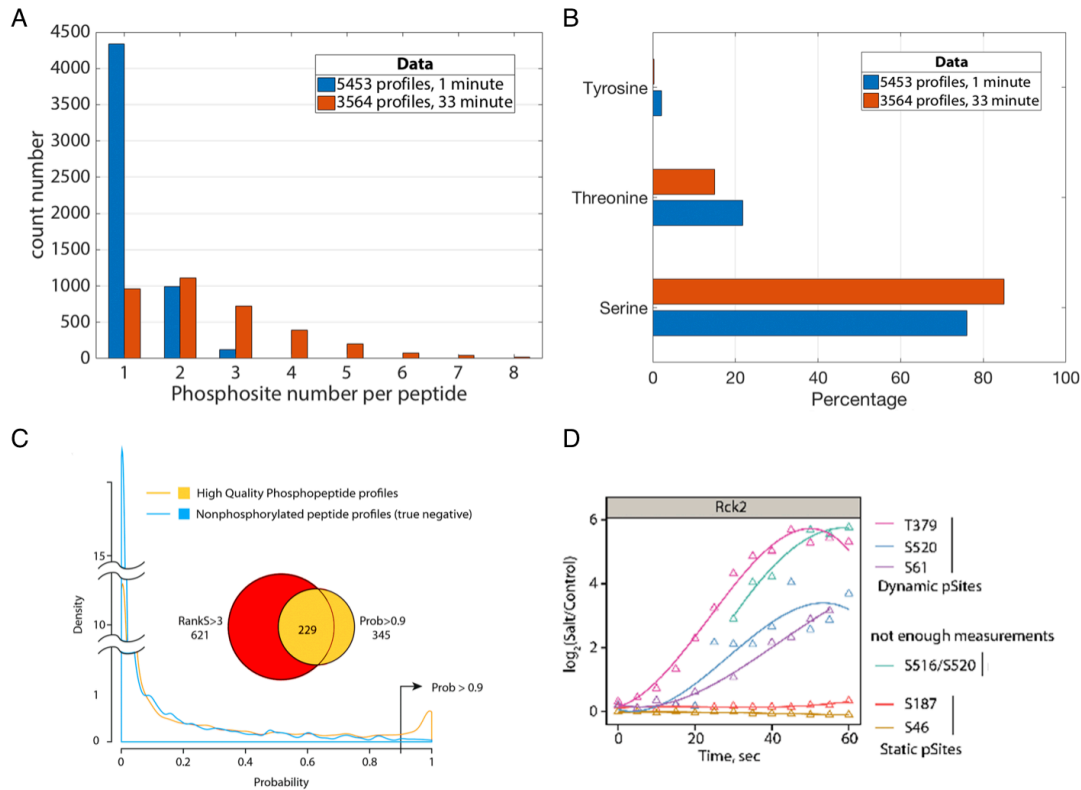
Figure 5: Creation of high confidence temporal profiles.

(A) Sub-minute phosphoproteomic data reveals 80% of high confidence profiles consists of mono-phosphorylated peptides. In contrast, ~90% of the 33-minute phosphoproteomic data consists of phosphorylated residues equal to or less than 4. (B) Data for both timescales reveal serine residue beings phosphorylated the most, with ~80%. Threonine follows with 19%, and tyrosine with 1%. (C) Density distribution of up-down analysis applied on 5453 profiles (yellow circle), add a further 116 temporal profiles to selected data. (D) An overview of dynamic profiles, static profiles and incomplete profiles.

The enriched phosphopeptides obtained were analyzed by a LC-MS/MS using a nanoflow HPLC (Method Section 2.8). The sub-minute response created a total of 1,507,689 spectra. Among this, 582,259 spectra were uniquely identifiable, with a false discovery rate of 1%. These spectra belong to a total of 14,206 unique peptides, which

represented a total of 2,419 individual proteins. From these unique peptides 5,453 high confidence temporal profiles were created, belonging to 1653 proteins. This procedure was also employed on Mascot Percolator for the 0-33 minute response data. As a result, a total of 3,564 high-confidence temporal profiles were created, belonging to 1238 unique proteins.

There were in total 3 criteria used in the making of the 5,453 and the 3,564 high confidence temporal profiles, in Kanshin & Bergeron-Sandoval *et al.* 2015 [26], and in this study. In order to have a good temporal profile coverage, each profile would at most have 3 missing FC measurements. Each profile would need to have a phosphosite localization confidence greater than 0.75 probability, and each FC value in a temporal profile would have a FDR less than 1% at both peptide and protein levels (Method section 2.9). A few examples of dynamic, static and incomplete temporal profiles are illustrated in Figure 5D.

The majority of the peptides from the sub-minute response would yield a mono-phosphorylated peptide. Whereas, in 33 minute response, there were significantly more double, triple and quadruple phosphorylation (Figure 5A). The amino acid that was modified the most was serine on both timescale (Figure 5B).

However, a further selection was made from the created high confidence profiles. This was to ensure that each selected profile would represent a rapid phosphorylation or a rapid dephosphorylation event. Selected profiles were referred to as either dynamic profiles or regulated phosphopeptide, which is used to distinguish them from static profiles. To discern these profiles, it was decided that a temporal profile would require at least 3 significant FC value (Method section 2.10). After applying this criteria only 621 temporal profiles were left for 0-60 second timescale (Figure 4C), and for 0-33min timescale there remained 1016 profiles.

However, this pipeline eliminates profiles that have small FC value; 89% of the profiles would be lost for the sub-minute response data. Therefore, to further select regulated profiles, in Kanshin & Bergeron-Sandoval *et al.* 2015 [26], an up and down analysis was employed. This analysis hinges on the notion that randomly fluctuating data are more likely to represent static temporal profiles [80]. Using this analysis 116 profiles

that were thought to be static were considered as dynamic (Figure 4C). As for the 0-33 minute response, a gradual thresholding on the FC values in combination with utilizing R^2 value were used as a criterion to select 917 dynamic temporal profiles (out of 1016). This selection method assumes that large FC values measured indicate a dynamic profile, unless R^2 value for the fitted equation were extremely poor –then it is discarded. This method gradually increases its stringency on the R^2 value for profiles that have lower FC values. A high R^2 value indirectly favors continuously increasing and decreasing kinetic profiles (Method section 2.11).

3.2 Dynamic phosphosites on the MAPK-HOG pathway upon osmotic stress

Osmotic shock has a profound effect on yeast cells. It causes temporary cell cycle arrest, influences endocytosis, alters transcription state, and impacts cellular morphogenesis. One particular pathway that is instantly associated with osmotic shock is the yeast HOG (High Osmolarity Glycerol) pathway itself.

On both timescales we found Hog1 residues at T174 and Y176 exhibited fast phosphorylation kinetics, Figure 6. These sites are known to activate Hog1 and cause it to localize to the nucleus. The cellular response to osmolarity starts as soon as 15 seconds after exposure to NaCl, Figure 6. A maximum FC of 64 was measured at the 5 minute. For this reason, sample preparation needs to be extremely fast. All regulated sites exhibited a sigmoidal shape. Interestingly, despite the fact that these phosphosites reached a maximum FC value within 0-60 seconds time interval, its maximum FC value was actually measured within the 0-33 minute time interval. Unfortunately, the mono-phosphorylated phosphosites, T174 and Y176, observed in 0-60 second timescale were labeled as di-phosphorylated by Mascot for the 0-33 minute timescale. Despite this, these kinetic profiles have similarities between these two timescales. Their FC value increases over time and remains mostly constant until the end of the experiment, just like seen in the sub-minute timescale. In addition, the 0-33 minute raw MS data for Hog1, indicated in blue and green (Figure 6), were identified to have a phosphorylation number of 1, and the top trace (red) had a phosphorylation number of 2. Due to these two reasons it was reasonable to assume that Hog1 over two timescales were comparable. It is thought that Y176 is contributing more than T174 for the kinetic profile labeled in green, and T174 was the major contributor to the kinetic profile labeled in blue. However, this is not known for certain. It is thought that

different oxidation identification by Mascot may have resulted in di-phosphorylation labelling of Hog1 for the halfhour timescale.

Upon osmotic shock, signals from osmosensors converge onto a scaffold/MAPKK Pbs2, and residues S514 and T518 are phosphorylated, which in turn activate Hog1. Our study also revealed that Pbs2 has a dynamic phosphosite at residue S514 on both timescales. A maximum FC of 6 was measured within 3 minutes and the FC remains mostly constant over the remaining 30 minutes, (Figure 6).

Some dynamic phosphosites were also found in the Sln1 and Sho1 osmosensing branches. Sln1 protein is an irregular kinase that can phosphorylate histidine residues. It acts on Ypd1 and Ssk1 through a two-component phosphorelay mechanism [96]. Our experimental setup was not configured to measure phosphate bonds on histidine and aspartate. Despite this, there were dynamic phosphorylation on regular residues (T, Y and S). A rapid Ssk2 dephosphorylation was observed at residue S118 in 0-60 second time interval, with log2 FC value of -2. This de-phosphorylation has continued on in the 0-33 minute time interval, reaching a minimum log2 FC value of -4. After 5 minutes exposure to NaCl, the de-phosphorylation value remains constant and does not significantly change. Interestingly, in regard to the continuity between two different timescales (0-60 second and 0-33 minute), the rapid phosphorylation of Ssk2 at residue S54/S57 switches to a rapid de-phosphorylation at the 0-33 minute timescale.

Sho1 branch has two sub-branches: the Hkr1 and the Msb3 sub-branch. The Hkr1 sub-branch is named after its osmosensor Hkr1 protein. Hrk1 is highly glycosylated and contains two extracellular domains responsible for activating Hog1. However, not much is known about this sensor. Two regulated sites were identified at S37 and at S139. Both of these kinetic sites were present in 60-second and 33-minute timescales. Interestingly S139 seems static at 60s timescale, but then undergoes a significant FC in the 0-33 timescale. This might be because it is di-phosphorylated, and S141 may be more important at a later time. These sites were not found in literature.

Bem1 is involved in cell polarity and morphogenesis and is bound to the intracellular domain of Msb2, recruiting the kinases Ste20 and Cla4 to the membrane. Either of these two kinases could be activating the kinase Ste11 [97]. Bem1 does not exhibit a strong FC within the first 60s at residues S48/S49/S50/T51, however few minutes after, a log2 FC of

2 was measured. This penta-phosphorylated peptide
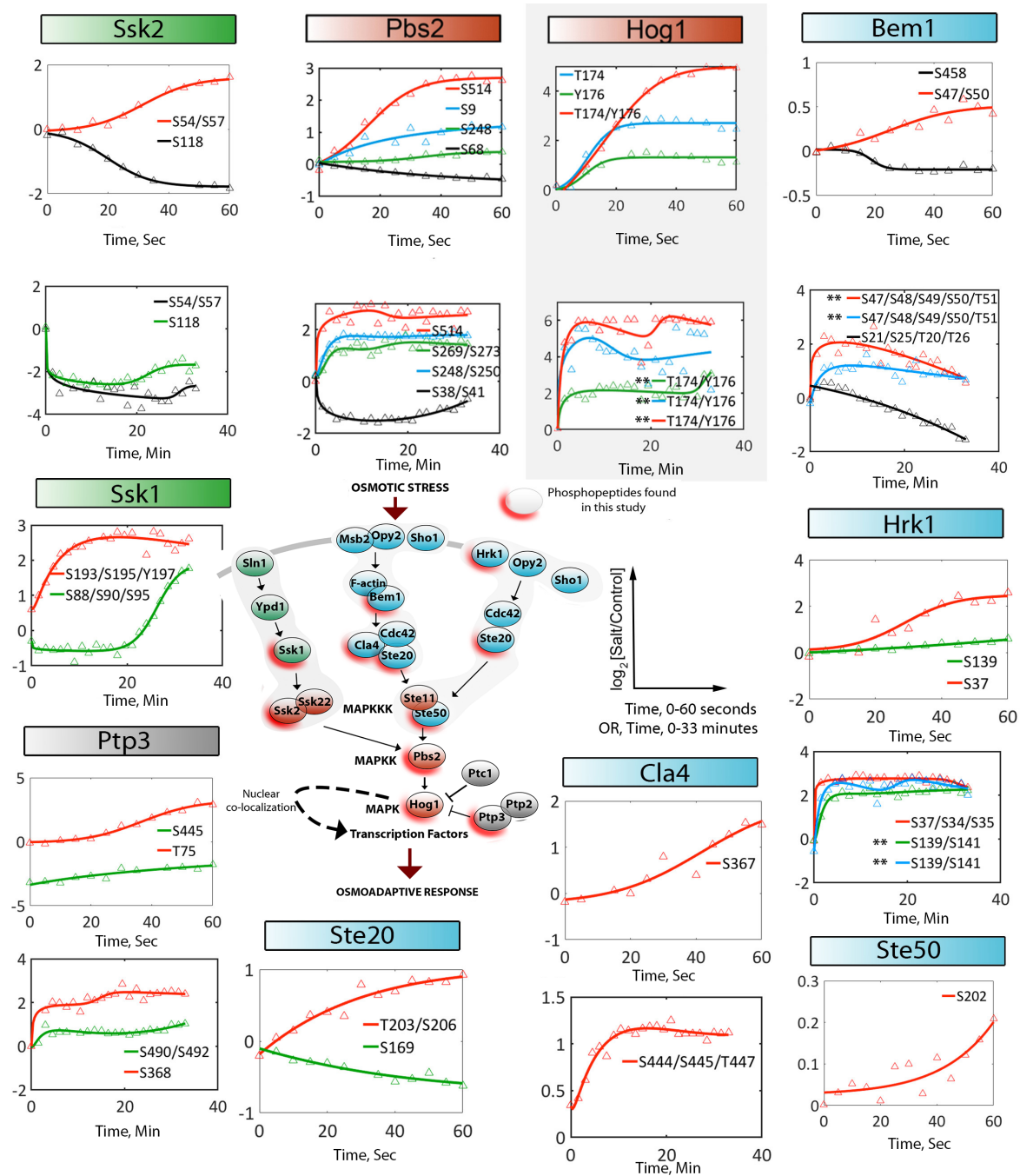
Figure 6: Dynamic phosphorylation of HOG MAPK pathway over 0-60 seconds and 0-33 minutes time frames
Schematic model of the Hog pathway is shown in the center. The Sln1 branch is shown in green and Sho1 branch shown in Blue. Sho1 branch is further divided into 2 as Msb2 and Hrk1 sub-branch, named after the osmosensing counterparts. Out of 21 proteins shown 11 proteins were present in either 60 second or 33 minute response data. These are underlined by a red shadow drop. Double asterisk (**) indicates independent kinetic profiles with different MS Mascot IDs, which are all di-phosphorylated.

also undergoes slow dephosphorylation over the 33-minute timescale. However, it is difficult to compare this peptide over two timescale as it is first di-phosphorylated and later it is penta-phosphorylated.

Changes in phosphorylation of both PAK-like kinases Ste20 (T203 and S206/S169) and Cla4 (S367 and S444/S445/S447) were also measured. However, we did not observe any dynamic phosphorylation on the MAPKKK Ste11, where both sub-branches of Sho1 converge.

Furthermore, a single dynamic phosphosite was recovered on Ste50, at residue S202. This was achieved by slightly relaxing the selection criteria for creating high-confidence dynamic peptides (described in method section 2.11). It turns out that residue S202 is reported to be one of the three phosphorylated residues with (S/T)-P consensuses. It is reported that this site maybe a substrate for either Hog1, Fus3, or Kss1, which arises from mating pathway cross-talk [98].

3.3 The role of TORC1 and TORC2 in osmoadaptation

Another SILAC phosphoproteomic study was done on Saccharomyces cerevisiae investigating hot-cold stress, Kanshin et al., 2015 [25]. In this study cells were exposed to stress over 22 minutes, which had a temporal resolution of 2 minutes. Interestingly, the main complex involved in the adaptation to hot/cold stress was identified to be target of rapamycin complex 1, TORC1 via Sch9. It is intriguing that some of the proteins involved in the adaptation to hot/cold stress were also the same proteins involved in the adaptation to osmotic shock. Furthermore, a significant number of phosphosites were found in both the osmoadaptation data and in the hot/cold adaptation data. These sites are highlighted with the asterisk in Figure 7, and their hot/cold responses are adapted and shown in Figure 8.
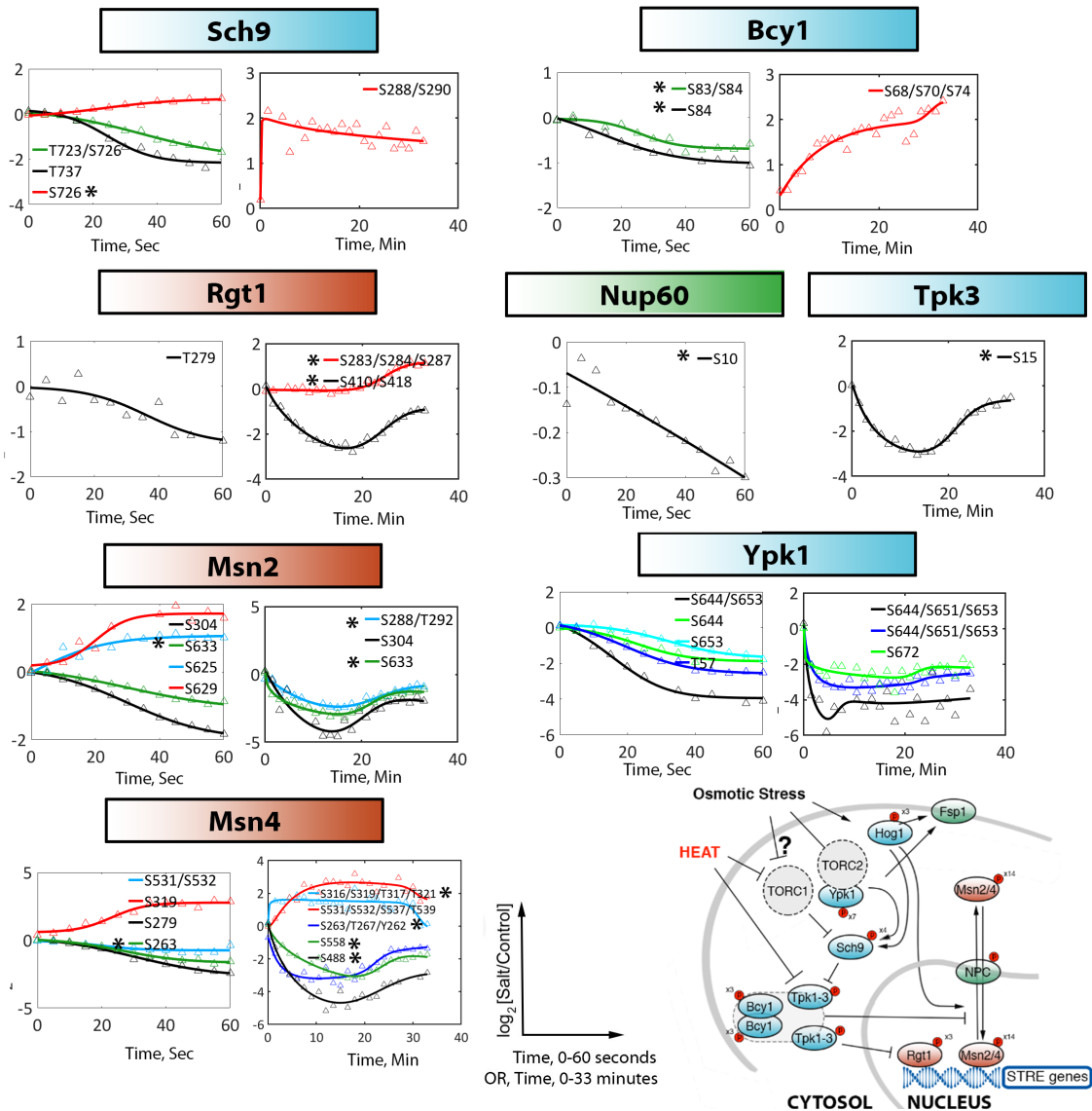
Figure 7: The possible involvement of TORC1 and TORC2 during osmoadaptation.
(A) Osmoregulated 8 proteins are curated. These proteins are also shown to be regulated as cells are exposed to hot/cold stress. Apart from Nup60 and Tpk3, every other protein has a dynamic phosphosites on both timescales; 0-60 second and 0-33 minute. (B) A model showing how TORC1 and TORC2 regulate Msn2/4. Because these proteins are regulated during osmotic shock, it is argued that these pathways may also be utilized during cellular osmoadaptation.

One striking outcome from the phosphoproteome study on hot/cold stress was that proteins were shown to be bidirectional. This means that either stress, hot or cold, would have its own unique response; either phosphorylation or de-phosphorylation. Some were found to be temperature independent (static), meaning that phosphorylation or

36

dephosphorylation was not observed regardless of the hot or cold exposure. Regulated phosphopeptides during the osmoadaptation process mostly resembled phosphopeptides response from cells that were exposed to heat. When osmoregulated phosphoproteins from 0-33 timescale are compared to the hot/cold stress, proteins such as Msn2 (S633, S288/T292), Msn4 (S263, S558, and 488), Nup60 (S10), Tpk3 (S15), Rgt1 (S410) and Bcy1 (S84 and S83/S84, for 60-second data) all underwent dephosphorylation. However, this does not account for every phosphopeptide; one of the main regulators, Sch9, exhibits a cold response kinetic at residue S726. Another cold response protein is Rgt1 (S283/*S284*/S287).
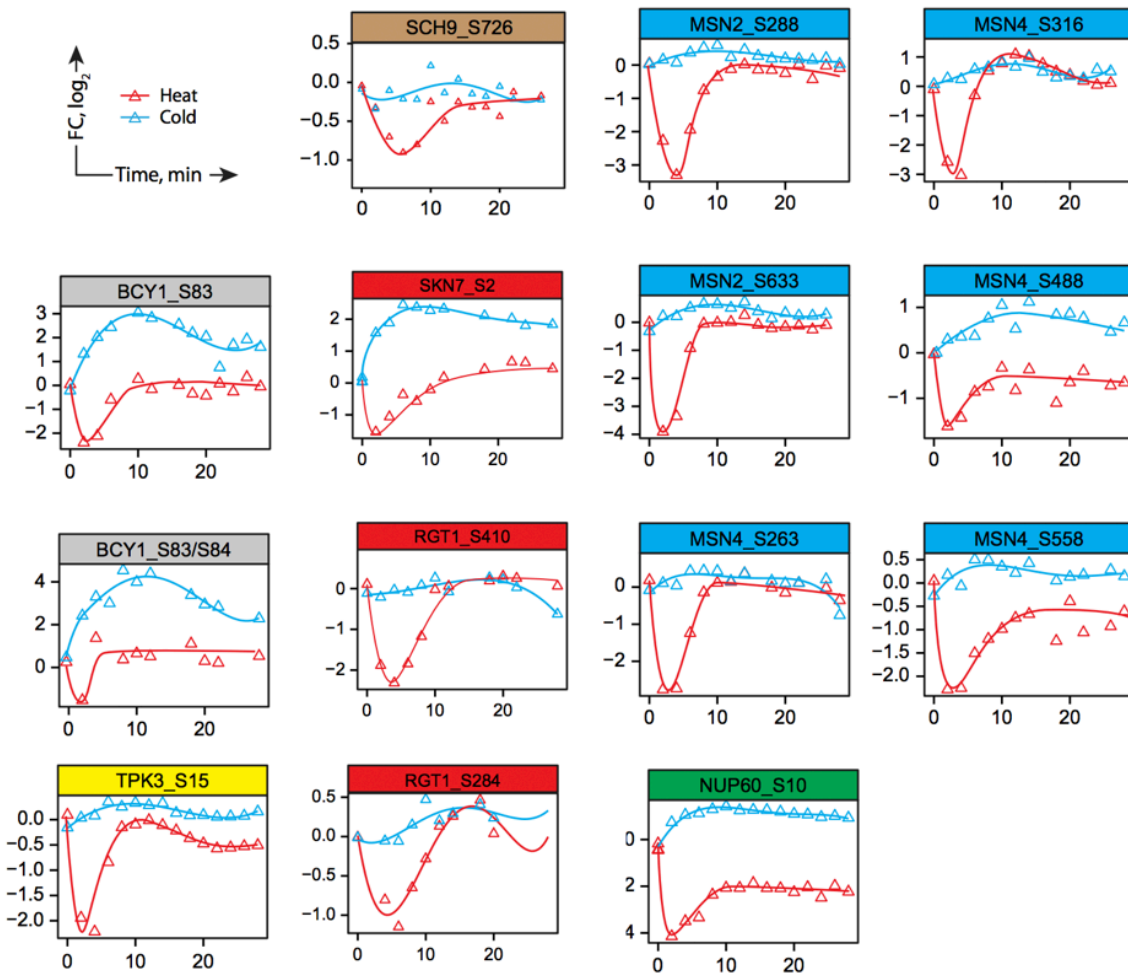
Figure 8: The phospho-kinetic profiles of budding yeast when exposed to hot/cold stress.
Kinetic phosphosites in response to hot (shown in red) and cold (shown in blue) that overlap with osmotic shock over a time period of 22 minutes, adapted figure from Kanshin *et al.,* 2015 [25].

It is striking to observe the extent of regulated phosphosites that are in common between osmotic stress and hot/cold stress. Furthermore, it is possible to state that heat stress is closer to osmotic stress in terms of the number of phosphosites that respond the same way.

In addition to the similarities of phosphopeptides between cold/hot and osmostress, another interesting protein identified, whose function was only recently elucidated, was the PhosphatidylInositol(3)-phosphate Binding, PIB2. PIB2 is involved in the activation of the TORC1 complex [99]. This protein is regulated in response to osmotic stress: there were two mono-phosphorylated residues at S113 and S381, which exhibited kinetic profiles on two timescales. Moreover, Pib2 had 7 dynamic phosphosite in 0-60 second time interval (Table 1).

3.4 Osmoadaptation regulating the canonical G1 checkpoint

Much work has been done to determine what constitutes the most up upstream activator of cell cycle entry in *S. cerevisiae*. The most upstream canonical activation of cell cycle is linked to the release of CLN3 mRNA from the Whi3 protein. This allows CLN3 mRNA to be translates and form the Cdc28/Cln3 complex, which in turn causes the cell to pass the G1/S cell cycle checkpoint (the START mechanism) [35][100][101][102]. However, we do not know what causes the release of CLN3 mRNA. Interestingly, osmotic shock regulates 67% of the proteins involved (6/9) in the canonical G1 checkpoint. These proteins have kinetic phosphosites in both 0-60 second and 0-33 minute timescales (Figure 9A). If we assume that what causes cell cycle to stop also takes part in its start, then some identified phosphosites could play a role in the cell cycle START mechanism. Since there are many proteins being regulated during osmotic shock, it raises the possibility that there may be more than one target that needs regulation simultaneously for cells to release the CLN3 mRNA from the Whi3 protein.

Within the first 60 seconds of osmotic stress an inhibitor of the cell cycle Whi5 is dephosphorylated at residue S88. The residue S88 is one of the 3 documented HOG1 phosphorylation sites [103]. At the 33-minute timescale no data is available for S88, but other phosphopeptides, including residues S161 and S154/S156 are identified to be de-phosphorylated and one peptide is tetra-phosphorylated at residues S59/S62/T57/T67.

Interestingly, in total, our study has picked up on the 6/12 known targets of CDK phosphorylation on Whi5 [104]. And T57 and T67 are among the new unreported sites that could play a role in the securing the Whi5 inhibition of the SBF complex (Swi6/Swi4/Stb1) that activates transcription.

Furthermore, within the 0-33 min timescale, Cdc28, a kinase known to drive cell cycle was identified to be regulated. The data indicates a gradual phosphorylation at residues T18/T19 that reaches a FC value of 2 at 28 minutes (Figure 9A).
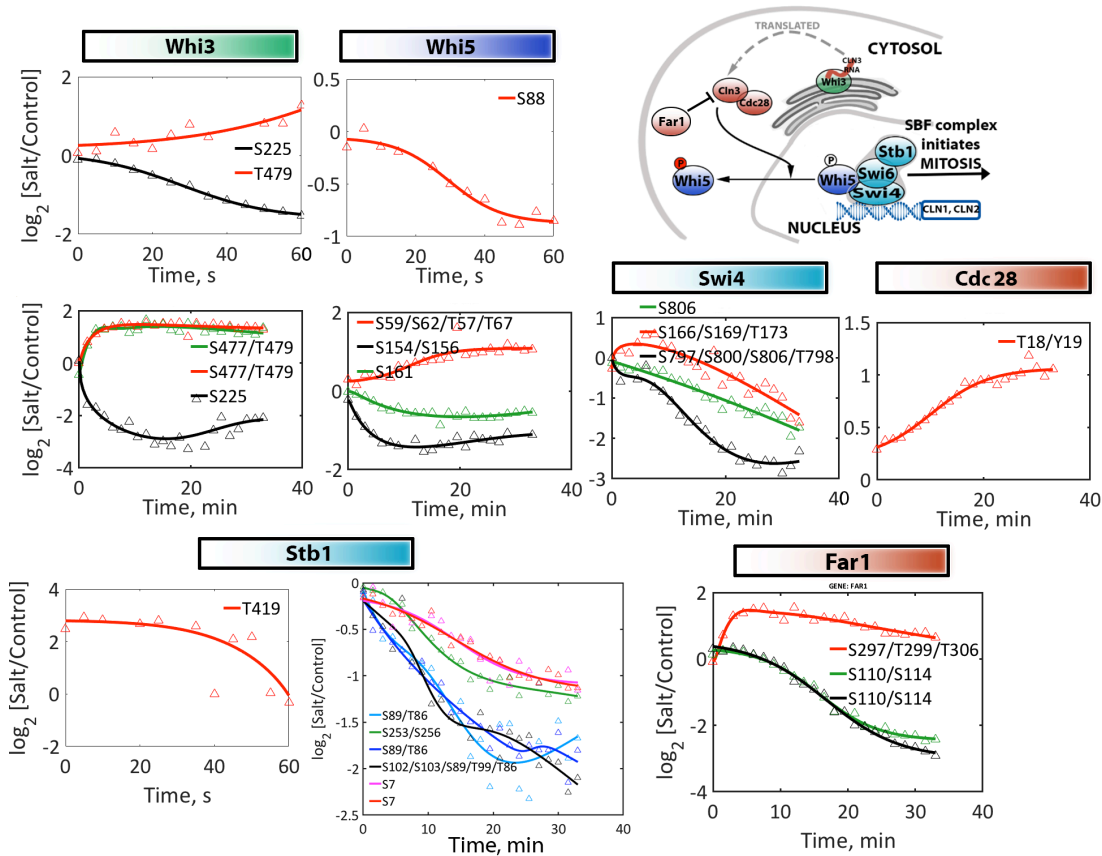
Figure 9: Majority of the cell cycle entry proteins are regulated in response to osmotic shock.
(A) Are some of the proteins that take a part in the G1/S transition for the cell cycle, which also have a dynamic regulated phosphosite. (B) Is the schematic of the major players of the G1/S checkpoint that initiate cell cycle.

Upstream of the canonical cell cycle driver, Cdc28-Cln3 dimer complex, is a CLN3 RNA binding protein Whi3. This protein is known to sequester the CLN3 mRNA to the ER via its polyQ track [105]. In addition, Whi3 is also a target of Cdc28, and is capable of binding to mRNAs of 262 genes [100]. On both time intervals, the 0-60 seconds and the 0-

33 minute, a consistent dephosphorylation of Whi3 at residue s225 is observed (Figure 9A), and a steady state in the FC is reached after 10 minutes of stress. The position of the regulated phosphosite is between Cdc28 interaction domain, 121-220, and polyQ track, 247-277, which could serve as an important modulating site for the sequestration of CLN3 mRNA to the ER. The residues T479 and S477/T479 are also regulated and these sites are closer to the N-terminus where an RNA binding domain is present. A steady state in FC is reached within first few minutes. All 3 dynamic phosphosites have been confirmed by other mass spectral studies [106].

Interestingly, contrary to expectations, a MAP kinase Slt2 that activates a subset of G1/S-regulated cell wall biogenesis genes through its physical association with and phosphorylation of SBF [107] showed no differential phosphorylation (static). However, the pheromone-activated CDK inhibitor Far1 was identified to be regulated. It is unclear if this serves as a feedback mechanism ensuring a robust response or a cross-talk between mitogen response pathways.

3.5 Global dynamic properties of osmotic shock in sub-minute and 33-minute timescales and activation of HOG signalling.

Global dynamic peptide properties of kinases and phosphatases were examined using a fuzzy c-means clustering. The 0-60 second experiment results were grouped into 6 distinct clusters. These clusters were sufficient to represent most of the kinetic profiles (cluster membership > 0.5, Methods 2.12, Table 1). In total 596 (81%, 596/737) profiles were clustered. There were 112 unique genes that populated phosphorylation clusters, 168 unique genes that only populated de-phosphorylation clusters and 55 genes had mixed properties (Figure 10A-9B). The mixed group includes proteins like Whi3 and Sla1 (Figure 10B).

Sla1 is an endocytic protein known to physically interact with 20 other kinases and 2 phosphatases (Biogrid). Among them are 7 kinase, Akl1, Cdc28, Prk1, Rck2, Cbk1, Bck1 and Pkc1, and one phosphatase, Ppz1, that was shown to be regulated. Similarly, Whi3, an mRNA binding protein, involved with G1/S cell cycle checkpoint, is known to physically interact with 15 kinase and 3 phosphatases (Biogrid). Among these interactions are 7
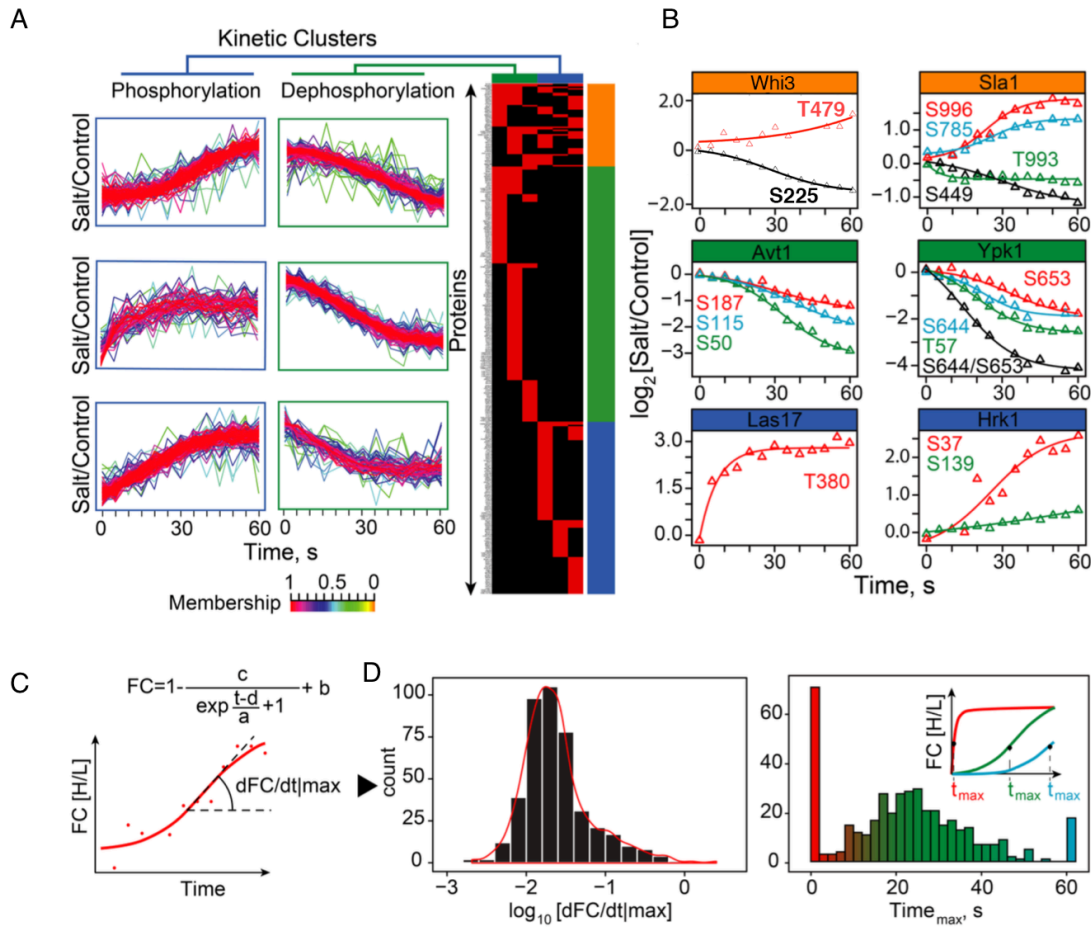
Figure 10 | Global kinetic analysis of signalling response, sub-minute study.
(A) Fuzzy c-means clustered regulated peptides into 6 distinct kinetic profiles (left panels). The cluster membership of the kinetic profiles are represented by color code (right panel). There are 596 dynamic phosphosites having a membership value above 0.5, displayed as a heat map. Peptides were either phosphorylated (blue box), dephosphorylated (green box) or both (orange box). These dynamic sites belong to 332 distinct proteins (B) Examples of regulated phosphosites sites from each group are presented. (C) Fitting of kinetic profiles to a reverse fermi Dirac function enabled the extraction of maximum rates of Fold Change (dFC/dt_{max}) (right panel), as well as times at this occurred (t_{max}). (D) The distribution of the rates (dFC/dt_{max}) from the 596 dynamic sites on a log_{10} scale are shown (left panel). 68% per cent of maximum rates of Fold Change fall within one order of magnitude 72.5% of clustered profiles are sigmoidal in shape (see Figure 11) and reach t_{max} within a time window of 60 seconds (green bars in right panel). No sigmoidal-like profiles reached t_{max} at 0 or 60s (respectively represented as red and blue bars) in contrast to exponential or linear-like profiles. See also Figure 11 and Table 1. Modified from Kanshin & Bergeron-Sandoval *et al.,* 2015 [26].

41

kinases, Cla4, Fpk1, Ksp1, Swe1, Tpk3, Cdc28 and Kic1, and one phosphatase, Msg5, were discovered to be regulated during osmotic shock. There are few new potential candidates that could regulate Whi3 and Sla1, at the residues shown in Figure 10B, upon osmotic shock.

To characterize the temporal nature of phosphorylation and de-phosphorylation of peptides, a simple reverse Fermi-Dirac function was empirically fitted (Figure 10C). Two parameters were extracted from the fitted equation: maximum rate of FC corresponding to an increase or decrease in phosphorylation (dFC/dt_{max}), and the time at which the maximum rate was observed (t_{max}) (Figure 10D, Method 2.11, Table 1).

The clustered profiles describing the sub-minute study were remarkably simple. The very first moments of peptide phosphorylation are measured in this timescale. The kinetics of the phosphosites that were discovered was either sigmoidal, linear or exponential. Notably, 72.5% of dynamic profiles were sigmoidal in shape (Figure 11), and most profiles approach their maxima (or minima) within 60 seconds (Figure 10D right panel). Considering that it was possible to characterize the kinetics into 3 distinct response curves — and 6 if we consider phosphorylation and dephosphorylation— it was quite elegant to only have high resolution that would capture the first moments of kinase activity and regulation. However, there were some profiles (114 in total) that did not cluster and there were discarded in Kanshin & Bergeron-Sandoval *et al.,* 2015 [26].

Notably, 98.5% of maximum change (FC_{tmax}) values were all within 2 orders of magnitude and 68.3% of these rates fall within 1 order of magnitude (Figure 10D left panel). This is an interesting finding as one could expect reaction rates of kinases and phosphatases to have a broader distribution due to differences in substrate abundance, subcellular localizations, complexes and other physical characteristics.

The landscape of the phosphosites kinetics on the 0-33 minute timescale was more complex. For example, a regulated peptide could start with phosphorylation, and there would be enough time to also observe its dephosphorylation. This was something that was not observed in 0-60 second time interval. Thus, because the longer timescale was more complex in terms of kinetic profiles more clusters groups were needed; in total 15 clusters

were required to represent the majority of the data, (Figure 12B). Some notable genes that exhibit a complex kinetic profile encode a protein involved in mRNA decapping, Not3 at residues S450/S454, and a polyamine transporter, Tpo3 at residue S55 (Table 2). These phosphopeptides are present in the 0-60 second and the 0-33 minute time intervals and were either be phosphorylate then dephosphorylated or vice versa.
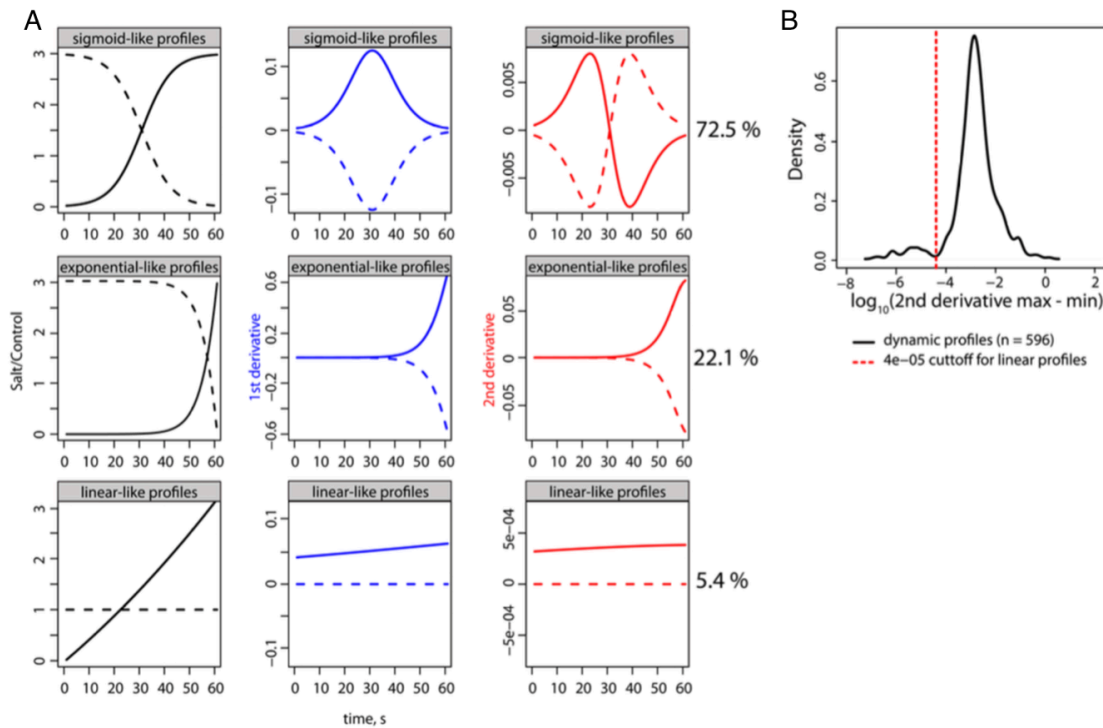
Figure 11: Analysis of the 6 kinetic profiles used for clustering sub-minute responses.

(A) Reverse Fermi-Dirac equation resulting in sigmoid (top), exponential (middle) and linear (bottom). Dashed lines are indicating dephosphorylation. The first derivative is shown in blue and second derivative shown in red. The shapes were sorted according to second order local max and min values and max-min difference. The occurrence of these shapes in the dynamic profiles is indicated on the right as a percentage. (B) Distribution on a $\log_{10}$ scale of the second derivative max-min difference for the dynamic profiles. We determined a cut off of 4e-05 for the max-min difference to sort linear-like profiles.
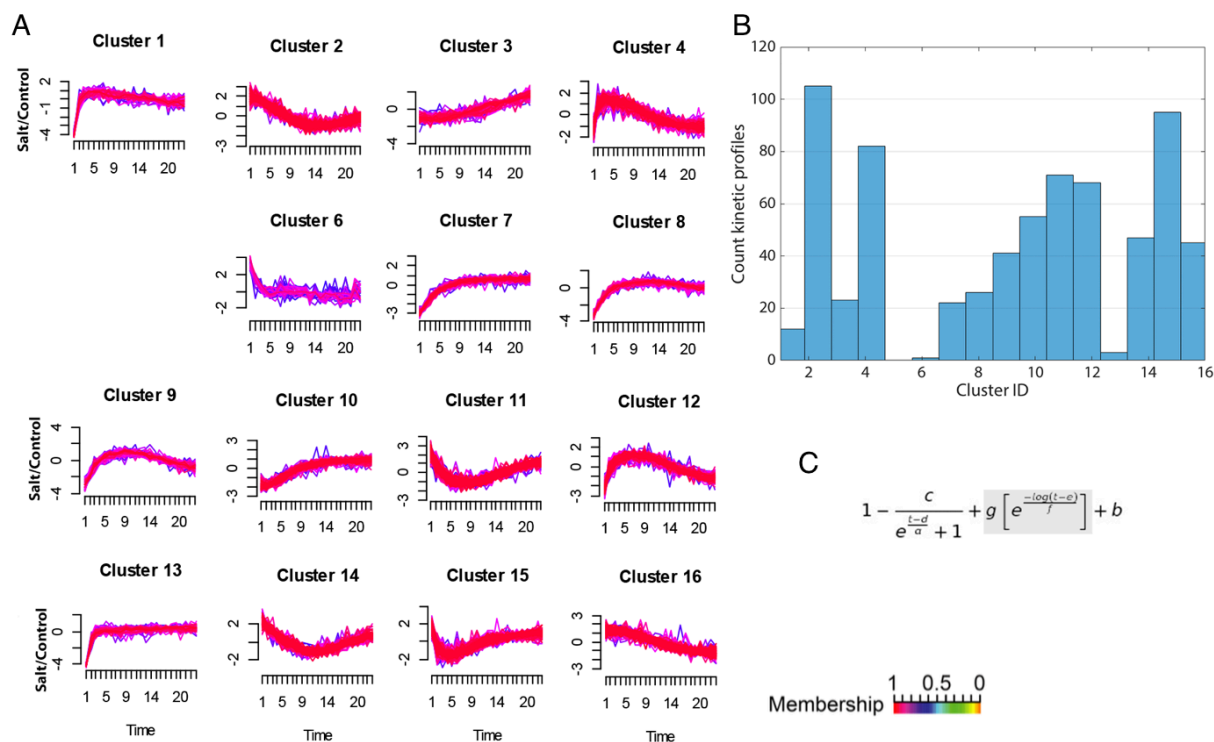
Figure 12: Global kinetic analysis of signalling response, half-hour study.
(A) 696 regulated peptides were clustered into 15 distinct kinetic profiles using fuzzy C-means (cluster membership > 0.7). These dynamic peptides were from 405 distinct proteins. (B) Is the occupancy of the cluster IDs; IDs 2, 4 and 15 had the highest occupancies, with more than 80 members each. (C) The reverse Fermi-Dirac equation with the added term (shown in grey) was used in the fitting of each temporal profile (Method 2.11 and Method 2.12).

The function used for representing the data over the 0-33 minute timescale was also a reverse Fermi-Dirac function, but with a single added term highlighted in grey (Figure 12C). This term would help the function accommodate the switch in regulation (i.e. Figure 12A, cluster ID 4, 12 and 14). In total 696 (76%, 696/917) regulated phosphosites were clustered (cluster membership > 0.7). These clustered peptides belong to 405 unique proteins (Figure 12A). The most populated IDs were 2, 4 and 15. These clusters respectively illustrate the rapid sub-minute phosphorylation and a gradual de-phosphorylation (ID 2), slower phosphorylation and a gradual de-phosphorylation (ID 4), and sub-minute phosphorylation followed by fast de-phosphorylation and a gradual phosphorylation (ID 15).

For determining the dynamics of phosphopeptide, only clustered profiles were selected as dynamic profiles in the sub-minute data (Kanshin & Bergeron-Sandoval et al., 2015 [26]). This was not applied for 0-33 minute data because peptide profiles were more complex in 33-minute study and cluster size was empirically chosen to maximize data coverage. Even though there were 696 profiles clustered within 15 clusters, the dynamic profile number was 917 (Method section 2.10, Table 2).

3.6 Dynamic phosphorylation suggests a dense kinase-phosphatase network

The origins of signalling becomes exponentially more complex as it propagates over time because cells exhibit promiscuous phosphorylation, cross-talk together with the main stimulus specific main response (Figure 13A). In light of this, it was initially hypothesized that the main stimulus specific response was carried by the KP network. Therefore, the KP network was assumed to be faster compared to the more disorganized signalling cascade, which is a combination of cross-talk and promiscuous interactions. Indeed, the entire sub-minute regulation data, consisting of 5453 high quality profiles, supports the idea of networks become more complex over time. The number of phosphosites that were regulated within the first 5 seconds was 84, and it increases all the way up to 704 between 55-60 seconds (Figure 13B).
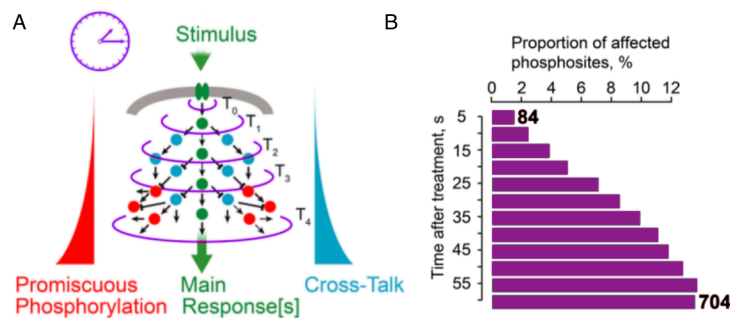
Figure 13: The origins of the signal propagation complexity.
(A) Propagation of signalling cascade causing a dense protein-protein interaction mesh (dark lines) composed of kinases and phosphatases (green and blue dots), which result in main and complementary responses to osmotic shock. We hypothesized that stimulus-specific signalling may occur faster than promiscuous signalling. (B) The global sub-minute response data showing the number of phosphosites that undergo a significant fold change (time at FC_{tmax}) increases over time (84 to 704 sites from 5 to 60 s after osmotic shock), adapted from Kanshin & Bergeron-Sandoval *et al.*, 2015 [26].

The kinetic profile over 0-33 minute timescale was more complex compared with 0-60 second data. To be able to compare kinetic phosphosites from both timescales the time at half maximum FC was extracted from each regulated profile. It was found that most of the kinetic profiles in 0-60 second data had a significant change in the FC at 20-35 seconds after exposure to stimulus (Figure 14A). The KPs corresponding to this data did not show a significant difference compared to the rest of the regulated phosphosites
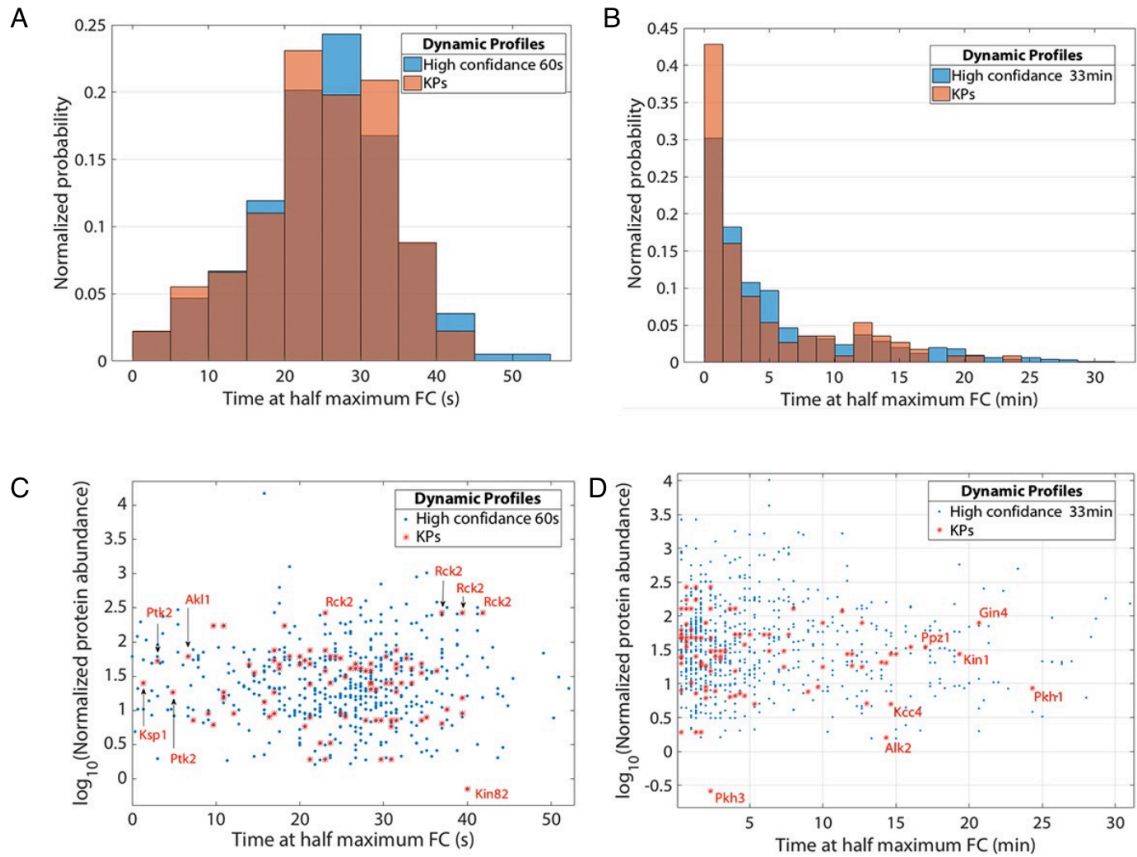
Figure 14: Protein abundance and time at significant FC for KPs vs non-KPs

(A) Is the normalized probability histogram indicating the time at which a significant change in FC has occurred for sub-minute data (596 profiles) and (B) 33 minute data (917 profiles). Both figures compare KPs with respect to the rest of the data. (C-D) Is the same data but compares them to protein abundance obtained from the Pax-db database [108].

(Figure 14A). Interestingly, for the half-hour data, most of the dynamic profiles did show a significant change within the first 3 minutes. Moreover, the KPs corresponding to this data, as opposed to the sub-minute data, were enriched for at 0-1.5 minute, when compared to the remaining dynamic data (Figure 14B). The probability of finding KPs does decreased after 1.5 minute of stimulus exposure. This probability does slightly increase again at 11.5

minute. This may be an indicative of the triggering of a second wave of KP activation. KPs found in the second wave are: Alk2, Cdc28, Fpk1, Gin4, Isr1, Kcc4, Kin1, Kin2, Ppz1, Prk1 and Prr1.

When cells experience osmotic shock a barrage of phosphorylation occurs within the first two minutes. Since abundant proteins are more likely to physically come into the vicinity of kinases, there is an increase in the probability that abundant proteins could skew the data. Therefore, we next wanted to examine whether there was a correlation between protein abundance and the time at which a significant FC had occurred. To that end, Figures 14C-D does not indicate any enrichment of abundant proteins being phosphorylated within the initial response. This result indicates that KPs and their substrates have enough specificity preventing non-specific (promiscuous) phosphorylation dominating KP activity.
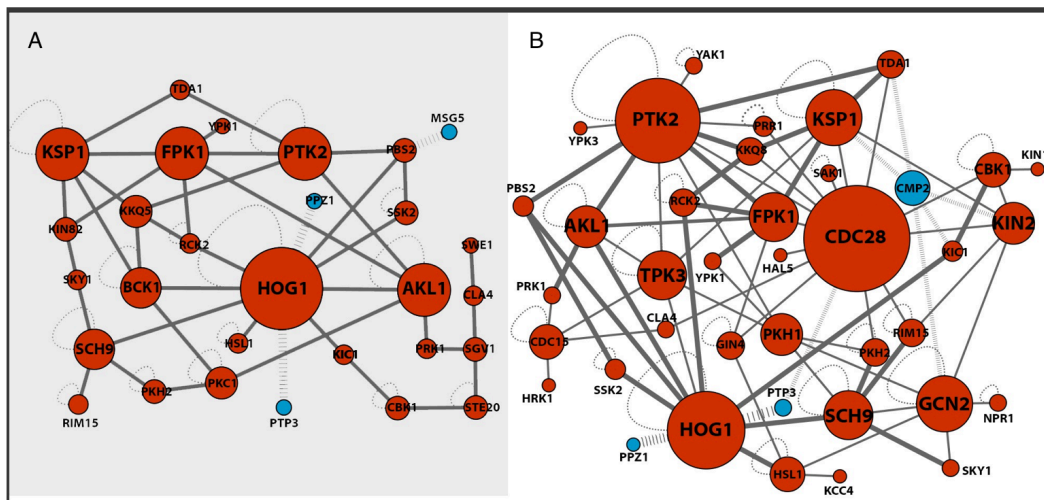
Figure 15: Physical interaction network of KPs, sub-minute and half-hour response.
(A) Physical interaction network of KPs that have a dynamic profile within the sub-minute response to osmotic shock. Size of the nodes indicates the number of interactions each KP makes. Red depicts kinases and blue depicts phosphatases. Hog1, Ksp1, Ptk2 and Akl1 are proteins that are connected the most. (B) Physical interaction network of KPs that have a dynamic profile in the 33 minute response to osmotic shock. Here Cdc28 overtakes Hog1 in terms of partners it has a potential to interact with. Bold interaction lines indicate the interactions present in sub-minute response, whereas the thin lines are new emerging interactions that are unique to 33 minute response. Physical interactions are obtained from BioGrid.

Saccharomyces cerevisiae has 129 kinases and 30 phosphatases in total, according to yeastkinome.org. From our MS analysis, upon exposure to high osmolarity, we found

24% (31/129) of kinases and 10% of phosphatase (3/30) had a dynamic profile within the sub-minute study. Furthermore, on the longer timescale (0-33 minute), we found 33% of kinases (43/129) and 10% of phosphatase (3/30) had a dynamic profile. The KPs that had kinetic profiles are highly interconnected, creating a dense interwoven interaction network. Approximately 85% (29/34) of the KPs in our sub-minute study physically interacted with each other (Figure 15A). Whereas, this number drops to 74% (34/46), for the half-hour study (Figure 15B).
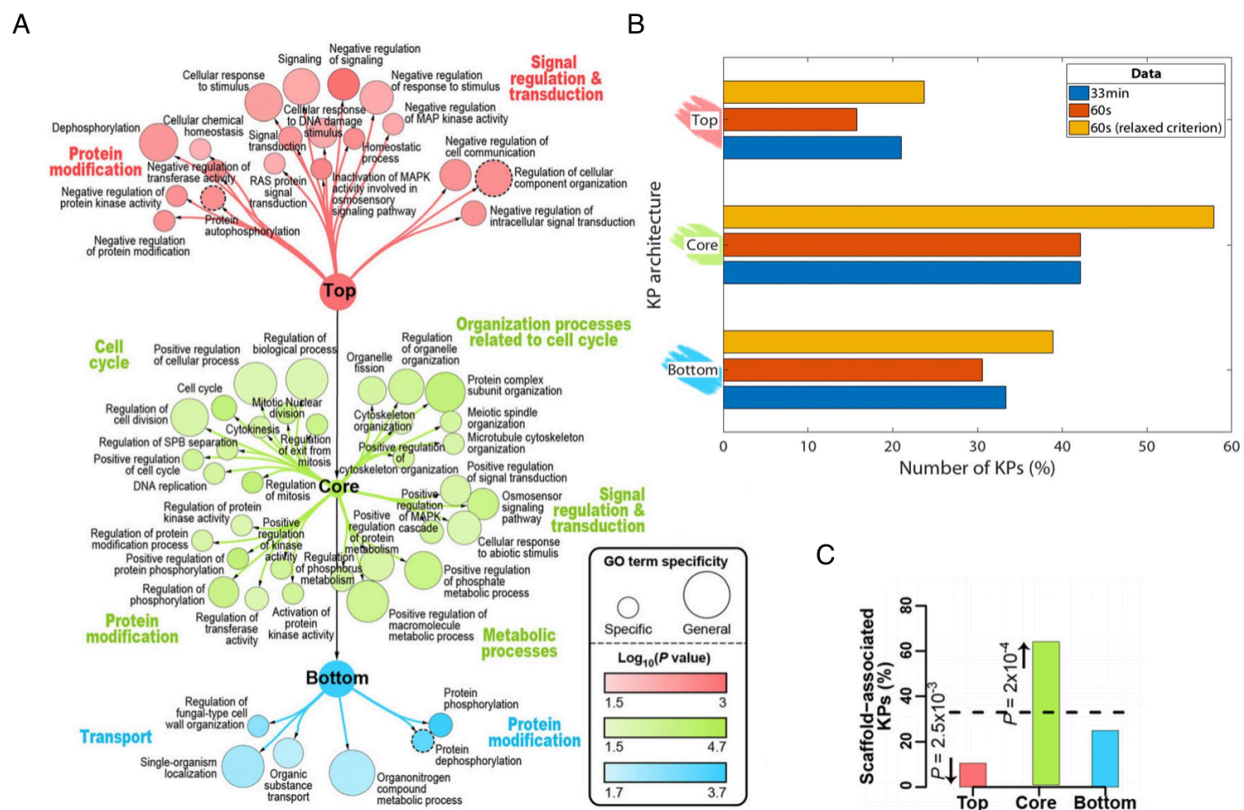
Figure 16: Dynamic KPs profiles mostly fall into the core component of the KP architecture.
(A) Indicate the functional GO terms enriched in the KP architecture diagram, adapted from Abd-Rabbo & Michnick, 2017. (B) 40% of the proteins that make up the core component have a high-confidence dynamic profile both in the sub-minute and 33-minute study. When high-confidence profiles are slightly relaxed, profile numbers increase and further populate the core component (Table 1). (C) Proteins that are scaffold-associated are enriched in the core level (adapted from Abd-Rabbo & Michnick, 2017).

Even though there is a slight reduction in the participation of KPs in the 33-minute response, the physical interaction network is clearly more dense and interconnected when compared

with the sub-minute network.

The total number of KPs that are regulated in *S. cerevisiae is* 159*.* Under stimuli-specific conditions, the KP interaction networks can be represented by Figure 15. It was hypothesized that regulated KPs could have similar topological network properties between themselves. To determine this these 159 proteins were projected to a KP architecture curated in Abd-Rabbo & Michnick*,* 2017 [64]. The core level, in this architecture, has the least member count and highest node connection. Both studies, the 0-60 second and the 0-33 minute, are enriched in the core component. Dynamic KPs made up 40% of all the core members (Figure 16B). This was not very surprising since the GO enrichment of the core component indicates GO terms like osmosensing, cell cycle, activation of protein kinase activity, bud neck, and positive regulation of MAPK cascade (Figure 16A). Furthermore, one other unique property of the core components is that the proteins that make up this level are associated with scaffold proteins (Figure 16C). This possibly suggests that scaffolds could be one of the reasons why we only observe an order of magnitude of difference within FC_{max} values for the 68.3% profiles. As scaffolds bring together proteins that are shown to increase efficiency of PPIs. Moreover, core enrichment also indicates that osmotic stress triggers the decision-making step, and consequently control systems that have feedback features.

3.7 Genes and phosphosites commonly regulated in sub-minute and half-hour timescales

In Kanshin *et al.,* 2015 [25], proteins with regulated phosphorylation sites were used to make a protein-protein interaction network, curated using BioGrid. The network is divided into four distinct regions. These regions are

1. general stress response that included transcription factors Msn2 and Msn4, (shown in purple);
2. morphogenesis, polarization and septum destruction that included Cbk1, (shown in light green);
3. septin ring assembly, vacuole inheritance and cytokinesis, (shown in purple); and
4. actin cytoskeleton clathrin-mediated endocytosis (CME) that included Las17 and Pkc1 (shown in darker green), Figure 17.

To identify stimuli specific cellular responses the 0-60 second time interval was chosen rather than the 0-33 minute time interval. However, 0-33 minute data also seem to confirm a stimulus-specific response. Notably, 58% of the proteins with changes in phosphorylation in the sub-minute response also changed in the 33 minute time interval. Approximately 62% of the protein-protein interaction network curated in Kanshin & Bergeron-Sandoval et al., 2015 [26], from sub-minute data, bottom right panel of Figure 17, was also discovered in the 33 minute study, Upper left panel of Figure 17.
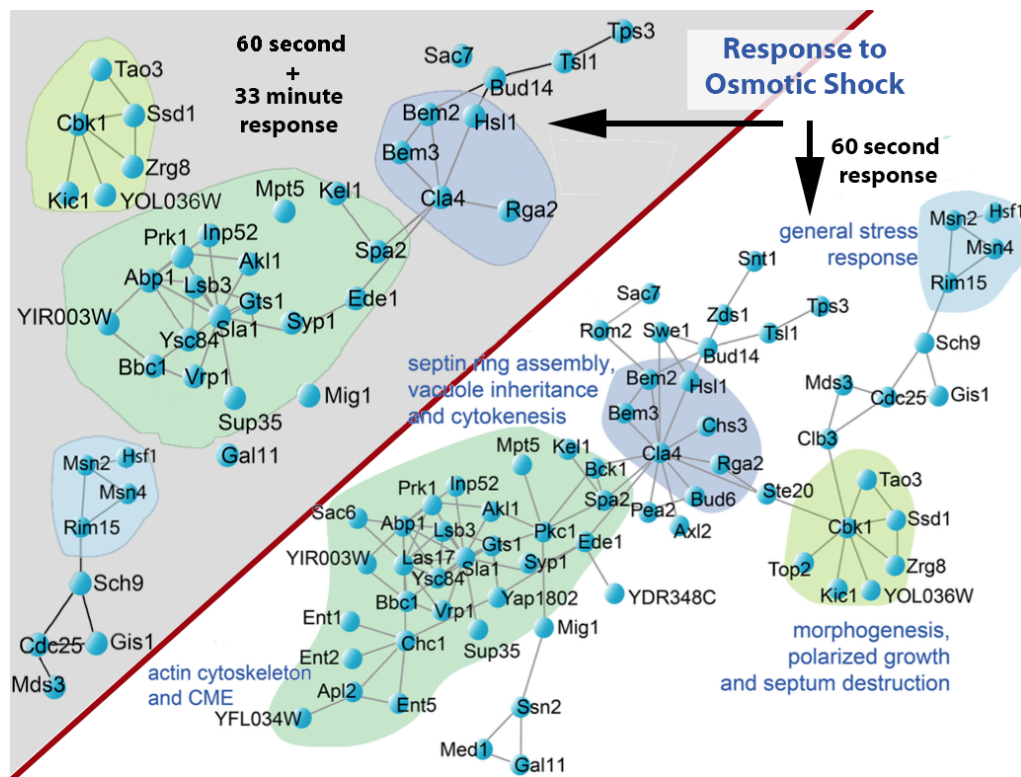
Figure 17: Protein-Protein interactions common between sub-minute and half-hour studies.
The protein-protein interaction network on the bottom right is curated in Kanshin *et al.*, 2015 [25]. The network presented on the upper left consists of regulated proteins from both studies (0-60 second and 0-33 minute time intervals).

In addition, there is a very good overlap of phosphosites between the two timescales. In total there were 161 phosphosites discovered that were regulated in both the 0-60 second and the 0-33 minute study (Table 3). These phosphosites belong to 100 unique proteins. A GO analysis was made on these 100 protein (Figure 18). Among the

161 dynamic phosphopeptide, only 45 were identical phosphosites; 33 sites were mono-phosphorylated and 8 were double phosphorylated (Table 3). The reason why the overlap drops was due to the fact that there were more multiple phosphorylated phosphopeptides found in the 0-33 minute data.
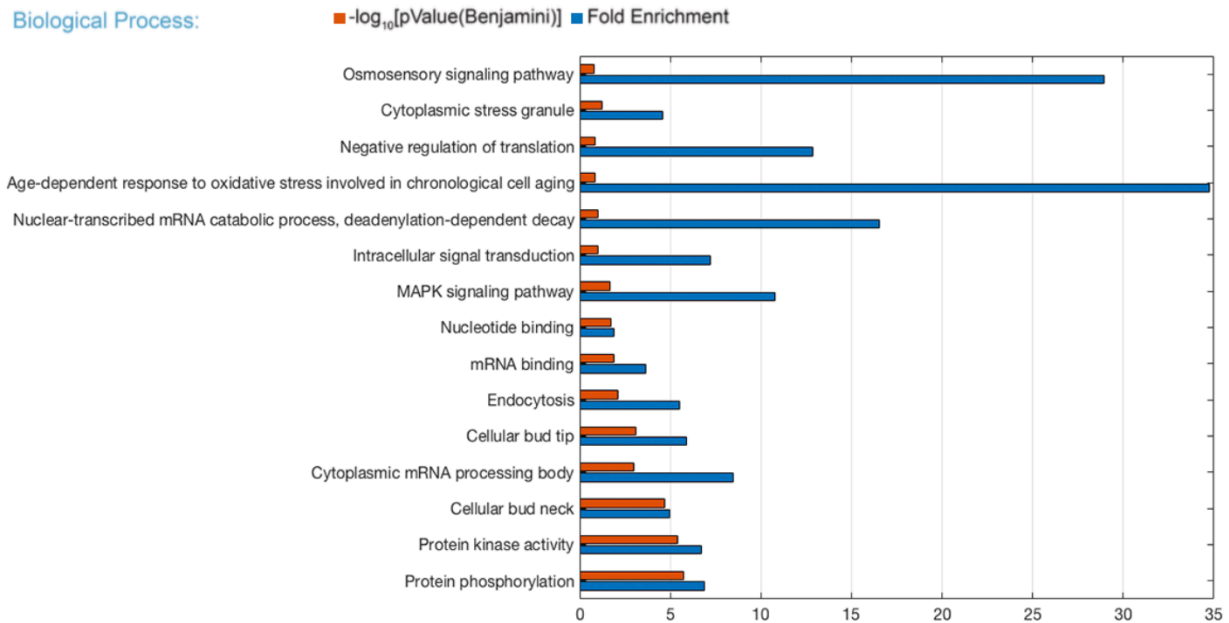
Figure 18: Go analysis on proteins that have conserved sites between sub-minute and half-hour studies.
Significantly enriched (P<0.01) GO terms among phosphoproteins containing dynamic phosphosites. Gene ontology enrichment analysis were performed with DAVID bioinformatics resources using the entire *S. cerevisiae* proteome as background.

The enriched GO terms show that the MAPK signalling pathway, osmosensors and endocytosis were still enriched in the 33-minute study indicating that proteins involved in osmotic stress would continuously need to be regulated and maintain an active state throughout the osmoadaptation process. This comes as no surprise as cell cycle only resumes after 74 minutes from exposure to high osmolality. After the more obvious GO terms, we found that cellular bud neck, cytoplasmic mRNA processing body, and cellular bud tip were among second most significant GO terms. Interestingly, mRNA binding proteins, stress granules and processing body GO terms were also enriched.

3.8 Proving causality between dynamic phosphosite and functionality

For some of the discovered dynamic phosphosites the causal relationship between the phosphosite and the osmotic shock was tested using cellular fitness assay. To maximize the sensitivity of this fitness assay, wildtype (WT) cells would be competed against their phospho-null counterparts. Replacing the phosphorylated residue with an alanine via site directed mutagenesis created phospho-null mutants, rendering this site non-phosphorylatable. Thus, competitive cellular fitness would measure relative growth under differential conditions.

In Kanshin & Bergeron-Sandoval *et al.,* 2015 [26], all the phospho-null mutant and WT cells were expressed from a plasmid flanked by native promoters and terminators [109]. Each phospho-null strain was also transformed with a plasmid coding for mCherry monomeric RFP and the wild-type strains with a plasmid coding for EYFP (Extended Experimental Procedures, Kanshin & Bergeron-Sandoval *et al.,* 2015 [26]). Growth competition assays began with equal numbers of mutant and WT cells. The competing cultures were maintained in exponential growth phase for 5 days. Population was once more adjusted to exponential growth pace and monitored over 120 hours. The population amplitudes were measured by fluorescence spectroscopy (Figure 19). Competition assays were performed in low fluorescence medium (LFM) or LFM medium plus 1 M NaCl to detect phosphosites that have impact on fitness in a different cellular context.

Proteins that are known to play an important role in response to osmotic shock are Hog1, Gpd1 (an enzyme responsible for the synthesis of glycerol) and Rck2 (a protein kinase involved in response to osmotic stress). Gpd1 S23A and S24 A showed growth deficit but the S27A mutant did not (Figure 19). This shows that Gpd1 S27A is not required in the osmoadaptive process. However, this site was shown to have a dynamic FC in our sub-minute response study (Figure 20A). The phospho-null mutants of Hog1, T174A and Y176A both had impaired growth compared to the WT, in both LFM and NaCl condition.

Rck2, which is activated by hyper osmotic shock and is a known substrate of Hog1 [29], surprisingly showed an increase in fitness for a T379A mutation. However, further study will be needed to determine why this happens.
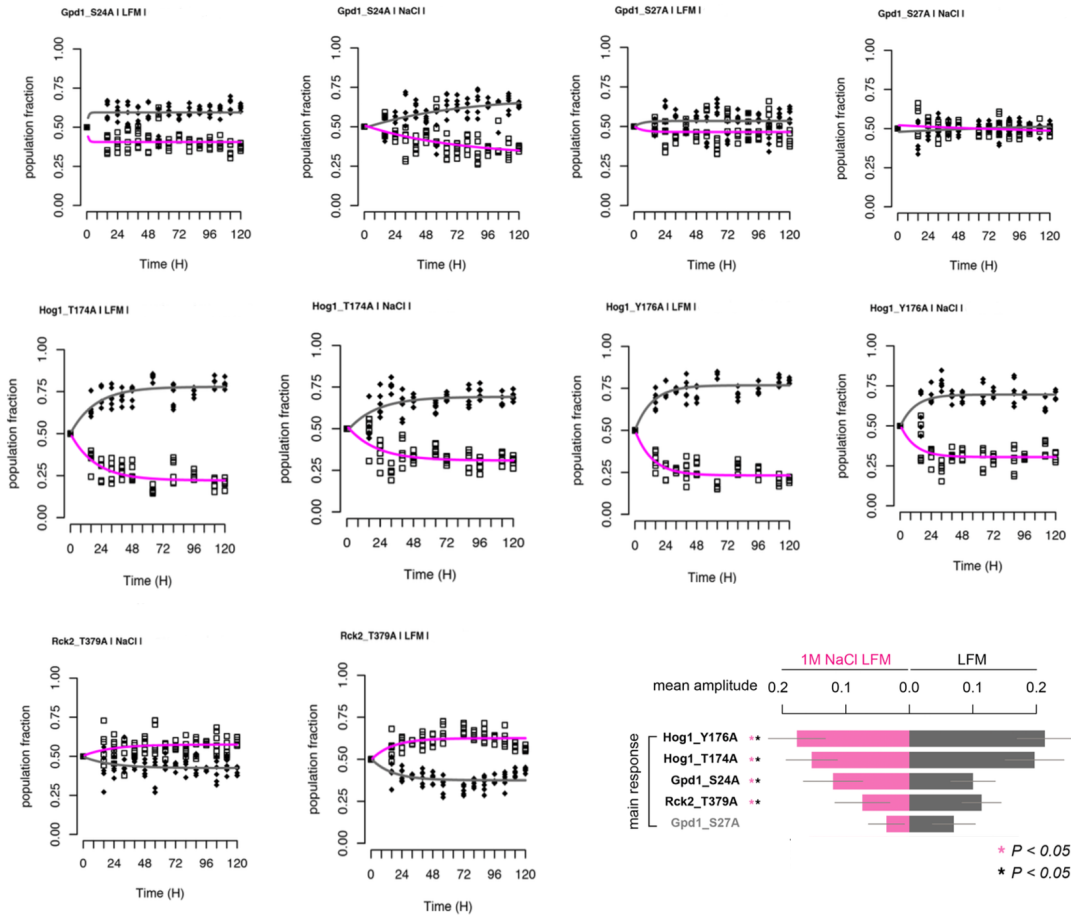
Figure 19: Fitness of phospho-null mutants was assessed by competition growth under high salt and non-stressed conditions.
Competition growth assays between mutants and their WT counterparts were made using specific fluorescent reporters. Phospho-null mutants where tagged with mCherry (empty squares and red curve) and the wild-type strains where tagged with EYFP (dark diamonds and grey curve) strains. Control assay (LFM) was performed using BY4741 strain expressing either mCherry or EYFP and were competed with its mutant counterpart to access normal population fluctuations.

53
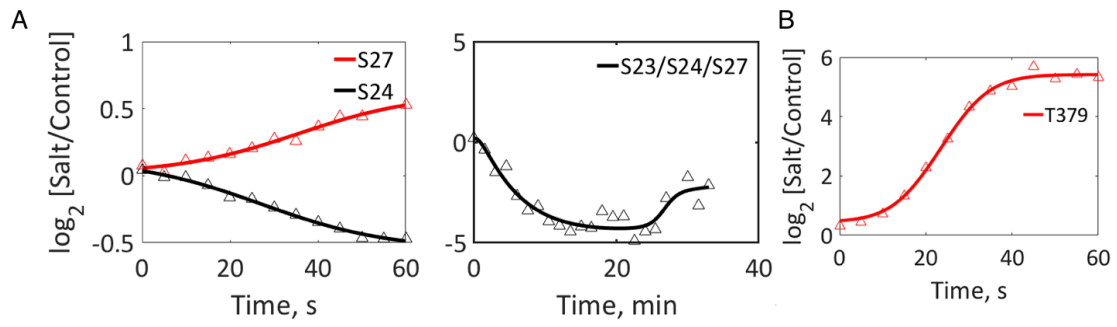
Figure 20: Dynamic phosphosites of Gpd1 and Rck2.
(A) Dynamic phosphosites on Gpd1 at sub-minute response (left panel) and at 33-minute response (right panel). (B) Dynamic phosphosites on Rck2 at only sub-minute response.

4. Discussion

The pipeline used for creating the temporal profiles for the 0-33 minute is very similar to that utilized in Kanshin & Bergeron-Sandoval *et al.,* 2015 [26]. However, phospho-kinetic profiles from the different timescales did not have the same amount of data point. Each temporal profile from the 0-60 second timescale had to have at least 10 FC value (out of 13), and for the longer timescale this number was 20 (out of 23). This difference affected the number of high confidence temporal profiles extracted. Consequently, we were able to generate more temporal profiles out from the 0-60 second timescale experiment (5,453 profiles), compared to the 0-33 minute timescale experiment (3,564 profiles). Surprisingly, there were more dynamic profiles found in the 0-33 minute time interval: 28% (1016/3564) of the data was considered to be dynamic, whereas this number was 13% (712/5453) for the 0-60 second time interval. In addition, a simple selection criteria were used for selecting dynamic profiles. These criteria utilized both FC values and R^2 values (Section 2.10). In spite of this the number of dynamic profiles that were clustered were about the same between the two timescales: 612 for the 0-33 minute timescale versus 596 for the 0-60 timescale. Due to the complexity of the dynamic profiles over the longer timescale, 15 clusters (Figure 12A) were used as opposed to 6 clusters that was used for the shorter timescale (Figure 10A). We did not discard dynamic profiles from the 0-33 minute time interval that was not clustered like in Kanshin & Bergeron-Sandoval *et al.,* 2015 [26], for the 0-60 second data. The amino acid that was most phosphorylated in both timescales were serine (~80%), this was followed by threonine (~19%) and tyrosine (~1%). Moreover, for reasons that remain unclear multi-phosphorylated peptides made up the majority of the longer timescale and mono-phosphorylated peptides were more prevalent in the sub-minute timescale (Figure 5A).

There are 25 proteins that make up the osmosensing branch and the yeast high osmolarity MAPK module. We were able to find phosphopeptides for only 44% (11/25) of these proteins. There were two reasons for this: first, the signal transduction did not all depend on S/Y/T phosphorylation; and second, trypsin digest did not produce >95% protein coverage for every protein. However, the main phosphosites that activate Hog1 (T174 and

Y176) were identified on both timescales. These sites were discovered to be phosphorylated within seconds after exposure to high osmolarity. On the longer timescale, we were able to show that these sites remained phosphorylates as long as 33 minutes, which was the duration of our experiment. These sites activate Hog1, and the activation is maintained throughout the experiment. Because yeast takes approximately 70 minutes to adapt to high osmolarity, it was not possible to conclude its deactivation with its dephosphorylation. Because the Hog1 phosphopeptides, in the 33-minute data, were di-phosphorylated (as opposed to mono-phosphorylation) it was difficult to directly compare them to the traces obtained from the sub-minute data. However, because these traces were very similar, it motivated us to look at Hog1 MS raw data for the 0-33 minute timescale. In Section 3.2, it was argued that Hog1 kinetic profiles within the sub-minute and the half-hour timescales were similar (Figure 6). Furthermore, Mascot identification of phosphorylation labeling has resulted in the assumption that one of the amino acid residue were more prevalent within the di-phosphorylated peptide. However, further verification is required to clearly show the mono-phosphorylated peptides from Hog1, for amino acids T174 and Y176, during osmoadaptation for the half-hour timescale.

The linear cascade shown in Figure 6 only represents a simplified model for the yeast Hog1 MAPK pathway. In reality, there are feedback control mechanisms that are in play that are used in the signal fidelity and robustness. Hog1 has been shown that it could regulate itself via phosphorylating the MAPKKK-Ssk2 at residues S54, S57, S68, S74, S78, T172, T178 and T194. We were able to capture 2 of these residues (S54 and S57), which was implicated in the fine-tuning of the basal activity of Hog1 for a successful osmoadaptation (Sharifian et al., 2015). Furthermore, Hog1 was shown to phosphorylate Ssk1, at residues S193 and S195, in vivo and in vitro (Sharifian et al., 2015). These sites were identified in the 0-33 minute timescale experiment. In addition, we were able to reveal other regulated phosphosites that have not been reported for Ssk1 and Ssk2 that could also contribute to the signal fidelity and robustness that could arise from a feedback control system during osmoadaptation. More recent studies have begun to distinguish differences in terms of how signal propagates in the Sln1 and Sho1 branches of the osmoadaptation process [34].

The MAPKKK-Ste50/Ste11 dimer that Sho1 branch converges to was not identified

in our study. However, when the stringency was lowered, we did discover one regulated site on Ste50 at residue S202. This site is one of the five MAPK consensus sequences (S or T followed by P). Furthermore, when Ste50 is digested with trypsin it produces two peptides that contain 21 serine (58%) and 11 tyrosine (50%), which are too large to detect using MS. In future experiments a protein of interest list should be created for the purpose of improving the protein coverage for these selected proteins. A complimentarily digestion to trypsin could vastly improve data quality and protein coverage.

Pbs2 does not seem to activate Hog1 via signal pulsing: a fast phosphorylation followed by a fast dephosphorylation. Like Hog1, it is probably continuously active throughout osmoadaptation process. The study by Granados et al., 2017 [34], has interestingly shown that modulating extracellular osmolarity influences the way cells respond. Future experiments could also test whether fluctuating extracellular osmolarity causes Pbs2 and Hog1 to have a different phosphorylation/dephosphorylation patterns during the osmoadaptive process.

The significance of HOG1 in osmoregulation is evident, however it should be noted that this is not an essential gene. Cells with *HOG1Δ* can still proliferate when exposed to 0.2M NaCl, and survive at 0.4M NaCl (Introduction 1.2). Cells are able to survive under high osmolarity most probably because there are other pathways that either work together with the MAPK-Hog1 or take over in the absence of Hog1. However, there are evidences pointing towards the importance of TORC1 and TORC2. Cells experiencing high osmolarity have TORC2-YPK1 kinase to modulate the glycerol synthesis and FPS1 activity [28][31][32][33]. In addition, the dramatic overlap of dynamic phosphosites between osmoadaptation and cold/heat stress was remarkable. There were 13 dynamic phosphosites that links the activity of TORC1 to osmoadaptation during both timescales (Figure 7 and Figure 8).

Some of the common transcription factors regulated in heat shock and osmotic shock are the following: Msn2 (S288 and S633) and Msn4 (S263, S316, S488 and S558). All these sites are located within PKA recognition motif. TORC1, known mostly for its role in nitrogen and amino acid starvation, could also be a candidate as an osmotic stress regulator [110]. TORC1 via an AGC family protein kinase, Sch9, is known to regulate the

PKA activity [111]. Furthermore, from the similar kinetic profiles in Figure7 and Figure8, it became evident that osmotic shock was closer to heat stress than it was to cold stress. Moreover, in support of this, Winkler *et al.,* 2002 [112] has also shown that heat stress can activate MAPK-Hog1. It is yet to be determined whether TORC1 is actively involved in the osmoadaptive response by stopping the cell cycle. One possible TORC1 substrate that could be involved in regulating cell cycle is the transcription repressor Dot6. This protein is a known substrate of Sch9 [113], and is reported to be a negative regulator of the cell cycle by means of ribosome biogenesis [114]. Our phosphoproteomic study has identified residues S313, S318, S322, S424, S313/S318, in Dot6, during the 0-60 second time interval, and five phosphopeptides S245/S247/S253/T251, S563/S569/S580, S321/S322/S326/S327/S331/T330, S281/S282/S296/S297, and S313/S318, in the 0-33 minute time interval to have a dynamic phosphorylation. Other notable substrates of Sch9 are Maf1, Stb3 and Tod6, which were also shown to have dynamic phosphorylation during osmoadaptation (Table1 and Table2) [111][115].

Another set of proteins that are candidates for regulating the cell cycle are the proteins of the G1/S checkpoint. Another reason to look at this phase is that G1 phase is by far the longest cell cycle phase in budding yeast. Therefore, it is more probable that phosphopeptides entering MS come from this phase. Cells exposed to high osmolarity temporarily stop cell cycle progression at the G1/S checkpoint [37]. We discovered that 67% of the proteins involved in the G1/S checkpoint have a dynamic phosphosite during osmotic shock. Because so many sites are simultaneously regulated, it is possible that the upstream components of the G1/S checkpoint do not constitute a linear signalling cascade. This would mean that the processing of the signal is more likely to involve feedback systems much like those seen in the Sln1 osmosensing branch. Furthermore, a linear signalling pathway leading to an RNA binding protein Whi3, resulting in the dimer kinase Cdc28/Cln3, which in turn releases the transcription inhibitor Whi5 from SBF factor, should in principle not depend on a bottleneck. If this were the case, this would make an organism very susceptible to random and deleterious mutations. If we assume that these discovered dynamic sites, which are responsible for stopping the cell cycle, are also regulating its start, then these sites can be used for designing experiments that help probe the kind of control mechanisms that take part in the START.

More specifically, Whi3 residues T479 and S477/T479 were identified to be regulated during osmoadaptation process. These sites are closer to the N-terminus where there is an RNA binding domain, which may be involved in the release of the CLN3 mRNA. This could potentially be an important post-translational modification for the START mechanism. In addition, it should be noted that the MBF transcription factor, known to be regulated along with SBF at the START, was not identified to be regulated in our study. This could be indicative that the regulation of the SBF transcription factor is sufficient for halting cell cycle.

Furthermore, a well know cell cycle kinase Cdc28, at residues T18/T19, was also identified to have a dynamic phosphorylation over 0-33 minute timescale. This site is significant as it is conserved from yeast to vertebrates. In vertebrates both sites are phosphorylated for full CDK activity [116][117], whereas in Fission yeast, a protein kinase Wee1 (homolog of Swi1) was shown to only phosphorylate residue T19 [118]. These phosphorylation sites are close to an ATP binding site. It was suggested that the activity on ATP binding site could be modulating the Cdc28 kinase activity [116].

Cells undergoing osmoadaptation must temporarily stop cell cycle. However, this does not necessarily have to be at the G1/S transition. Cells could also utilize other checkpoints such as G2/M checkpoint or spindle checkpoint to temporality stop cell cycle. Therefore, cells are likely to exhibit a heterogeneous response when exposed to high osmolarity, which is to some extent contrary to the genes under the control of general stress response element (STRE). For future experiments, it is important to consider the cell cycle synchronization of the budding yeast. This can be achieved by treating the culture with an alpha factor pheromone prior to osmotic shock. These experiments can improve our understanding of cell cycle specific STRE-regulated genes during the osmoadaptation process. These genes can be influential in determining pathways capable of temporarily stopping cell cycle and consequently cell cycle regulation.

To gain a more general perspective on the regulated phosphosites, we decided to cluster every identified dynamic phosphosite. In total there were 596 profiles that were clustered into 6 cluster groups for the 0-60 second timescale, and 696 profiles were clustered into 15 cluster groups for the 0-33 minute timescale. It is also very interesting that 98.5% of maximum change (FCtmax) values fell within 2 orders of magnitude, and 68.3%

of these rates fall within 1 order of magnitude for the sub-minute data (Figure 10D). The sigmoidal curve was the most observed response type (73%) in the sub-minute study (Figure 11). This kind of response may be a way to filter out high frequency noise caused by extracellular or intracellular origins. Furthermore, the sigmoid curve assures that any random, or short duration signals do not result in a cellular response. This kind of signal processing could prevent cells to respond incorrectly to an applied stimulus. A narrow range of rates could also favor an organization of enzymes and their substrates into complexes or physical localization to specific cellular compartments [119][120]. None of the traces exhibited dephosphorylation after phosphorylation or vice versa within the 0-60 second timescale, however in 0-33 minute timescale this was observed. The resolution in the 0-33 timescale was lower than the sub-minute study, 1.5 minute as opposed to 5 seconds. However, this temporal resolution was mostly sufficient for the half-hour study, except the very beginning. There was sufficient time to observe multiple phosphorylation/dephosphorylation events for phosphopeptides. It was interesting to observe the level of continuity in FC for every dynamic phosphopeptide. This feature of the traces raises our confidence that these data are not affected by random factors. In addition, there were some clusters, such as cluster ID 7,8 and 13 that had their FC reach to a maximum value and they remain mostly constant like those seen in Pbs2 and Hog1 (Figure 12A and Figure 6). These traces may be belonging to proteins that are constantly active during osmoadaptation, possibly within a complex or a cytoplasmic body. The maximum phosphorylation rates were not measured for the temporal profiles that were from the 0-33 minute timescale. This was because a significant number of dynamic traces could have multiple peaks and troughs that are more challenging to interpret.

KPs have a significant impact in regulating the cell; a recent study has estimated that KP's could regulate as much as 60% of all the budding yeast proteome [55]. This motivated us to examine the KPs with dynamic phosphorylation. The number of KPs that were regulated in the 0-60 second timescale was 34; 24% (31/129) of them were kinases and 10% of them were phosphatases (3/30). In the longer timescale (0-33 minute) the total number of regulated KPs increased to 46; 33% of them were kinases (43/129) and 10% of them were phosphatases (3/30).

It was hypothesized that the functional phosphorylation of KP-substrates occurs more rapidly following osmotic shock. These functional phosphorylations should overtake promiscuous phosphorylation arising from random PPIs that in principle result is a slower

phosphorylation rate (Figure 13A). For simplicity the time at which $FC_{max}/2$ was used over time at which maximum phosphorylation rate was observed ($Time_{max}$, Figure 10D). To examine this hypothesis, we extracted the time at which $FC_{max}/2$ was observed from both sub-minute and half-hour timescales. It was assumed that KPs would more likely form faster interaction networks among each other, much like in MAPK [65]. Contrary to these assumptions, we did not observe a difference between KPs and rest of the other proteins for the sub-minute timescale (Figure 14A). However, this was not the case for the 0-33 minute timescale. KPs were 15% more enriched when compared with the rest of the remaining proteins that were active within the first 1.5 minute (Figure 14B). Approximately 43% for KP's alone underwent dynamic regulation satisfying a significant FC of $FC_{max}/2$ within the first 1.5 minutes. This is another line of evidence that promiscuous interactions do not dominate larger timescales; relevant peptides undergo a significant FC at the beginning and not as much in the end. We also examined the correlation between protein abundance with time at which $FC_{max}/2$ was observed. However, it was found that abundance did not affect the time at which significant FC ($FC_{max}/2$) was measured. Thus, it led to us to conclude that KPs and their substrate have enough specificity, and that less abundant KPs were also regulated within the first minute of the 0-33 minute timescale. A similar finding was also reported in [121]. In line with this conclusion, regulated KPs were also more present in the core level (Figure 16B), and this level is associated with scaffold proteins, which could increase PPI efficiency.

With the longer timescale there were two concerns: (1) promiscuous phosphorylation out numbering relevant stimuli-specific phosphorylation modifications, (2) protein degradation or synthesis masking the post-translational modification. Although these two factors might have affected MS results, significant phosphoproteomic overlaps between the two timescales provides evidence that this is not the case. Furthermore, another phosphoproteomic study on budding yeast has also shown that protein abundance, over the 0-22 minute time interval, did not alter protein degradation significantly when exposed to cold/heat stress [25].

To further investigate how KPs could regulate themselves two KP interaction networks were created (Figure 15). There were two data used in the making of these networks: the proteins used had to have a dynamic phosphosite for that specific timescale,

and physical interaction between proteins had to be reported in Biogrid. The most connected node found in the sub-minute timescale belonged to Hog1. However, this was replaced by Cdc28 in the longer timescale. This could be indicative of how cells adapt to high osmolarity; Hog1 being responsible for the fast sensing and finer adaptation, and Cdc28 for stopping and adjusting the cell cycle.

Both of these KP interaction networks were projected on to a hierarchical KP structure made up of three layers (top, core and bottom), Abd-Rabbo & Michnick, 2017 [65]. As a result, both of these networks were enriched with the core layer (Figure 16B). This layer is enriched with proteins involved with scaffolds, and due to the bow-tie architecture, it is associated with feedback features and signal integrity.

It was initially thought that capturing early signalling events (phosphorylation or dephosphorylation) immediately after osmotic shock could only be possible for 0-60 second experiment. However, the constant FC observed for some significant proteins such as Hog1 and Pbs2, the enrichment of proteins related to osmoadaptation, and the protein abundance independent nature of FC values all contribute to the fact that stimuli-specific response can still be probed over the half-hour timescale. Furthermore, it is likely that stochastic interactions probably do not dominate these interactions due to a narrow FC rate observed in sub-minute timescale. Possibly proteins complexes, granules, and processing bodies and other liquid bodies also contribute to how cell swiftly adapt to stress. It is reported that yeast Hog1 is also sequestered in stress bodies and p-bodies upon high temperature stress [122].

The continuity of specific phosphosites between both timescales were also examined. There were 161 temporal profiles belonging to 100 proteins with at least one phosphosite in common. When we look at the number of proteins that were regulated in both timescales (not only matching phosphosites), this number increases to 332. However, because multi-phosphorylated peptides make up the majority of the data for the half-hour timescale, this resulted in the decrease of the exact phosphosite match to only 45 peptides (Table 3).

Furthermore, the phosphorylation and dephosphorylation of these 45 sites were investigated. The goal was to examine whether any discontinuity occurred in terms of phosphorylation becoming dephosphorylation or vice versa (switching) between the two experiments. Switching occurred mostly on phosphopeptides that had double-phosphorylation. There were 5 dynamic temporal profiles (out of 45) that exhibited switching, and four of them were double phosphorylated (total double-phosphorylated peptide number was 8/45). From MS data only, it was not possible to account for a mechanistic or a functional insight into this switching. This is because some proteins, such as Pib2, have only recently been studied, and for other proteins, such as Bem1, Swi4 and Not4, would require more dedicated experiments to be designed.

To further gain biological functions, a GO analysis was made on the 100 proteins that were shown to have regulated phosphopeptide during both timescales (Figure 18). Enriched terms such as MAPK signalling pathway, osmosensors and endocytosis were still present in the 33-minute study. This was also indicative of the fact that promiscuous phosphorylation were not dominating the half-hour experiment, and that meaningful and functional phosphorylations were measured.

5. Conclusions and Perspective

It is possible to gauge osmoadaptation processes from stimulus-specific measurements of phosphoproteome changes for short and longer timescales. Tandem mass spectroscopy (LC-MS/MS) was employed to measure phosphoproteome changes, which in turn reveal regulated phosphopeptides under osmotic shock. The goal of my memoir was to investigate osmotic shock and find proteins that were regulated by phosphorylation over on two different timescales.

Our study has discovered stimulus-specific regulation of proteins on two different timescales: the 0-60 second and the 0-33 minute. The method described and used demonstrates that minute amounts of cellular materials are sufficient for generating hundreds of stimuli-specific dynamic phosphosites. The data generated could serve as a stepping-stone to elucidate other less verified molecular pathways involved in cell cycle and osmoadaptive process.

There were 161 phosphopeptides that were regulated both in 0-60 second and in 0-33 minute time interval. This list of phosphopeptides made up almost ~30% and ~20% of all the dynamic phosphosites discovered within the sub-minute experiment and the 33-minute experiment, respectively. Other longer timescale experiments can also be found in the literature. One specific example was published in Kanshin et al., 2015 [25]. It examined the hot/cold stress on budding yeast over a 0-22 minute timescale. Interestingly, the hot/cold stress data also overlapped with our osmotic stress data that suggests the involvement of TORC1 in osmoadaptation.

Overlap between dynamic phosphosites associated with hot/cold stress and osmotic stress led to the hypothesis that pathways other than MAPK-Hog1 may be involved for the survival of S. cerevisiae in high osmotic stress. The fact that HOG1 gene not being an essential gene for the survival of S. cerevisiae also supported this hypothesis. In the future it will be interesting to exactly elucidate the cooperation between MAPK-Hog1 pathway and other complexes such as TORC1 and TORC2 in the osmoadaptive process. Some notable substrates that are regulated downstream of these complexes are Sch9 and Fsp1 (Figure

7).

During osmotic stress, cells temporarily stop cell cycle to divert its energy into adapting to the changing less favorable environment. This was the motivation when examining the G1/S checkpoint. Contrary to our expectations, 67% of the proteins involved in the G1/S checkpoint were discovered to have a dynamic phosphosite. Some of these phosphosites belong to Whi3, which is an RNA binding protein know to sequester a key cyclin, Cln3 mRNA, and Whi5, which is a cell cycle START transcriptional repressor. Cells do have other checkpoints, and these could also be utilized during the osmoadaptation process. However, because G1 phase is the longest cell cycle phase [35], it is expected that there would be more cells in this phase, which in turn increases the phosphopeptide count and MS data quality.

Moreover, the MAPK-Hog1 pathway was also examined on both timescales. Many of the proteins that was found to have a dynamic phosphosite in the sub-minute timescale also have a dynamic phosphosites in the half-hour timescale. It was initially assumed that larger timescales would be dominated by promiscuous phosphorylation due to the finite MS readouts (Kanshin & Bergeron-Sandoval *et al.*, 2015 [26]). However, the overlap between these two different timescales proves otherwise. Unfortunately, phosphosites T174 and Y176 were not discovered on mono-phosphorylated peptides for direct comparison. However, their response curves were similar: they remained mostly constant over the entire osmoadaptive process. In general, when gathering dynamic phosphosites, one difficulty to address is the causal relationship between kinase and its substrate. For example, it is not possible to clearly demonstrate which kinases directly regulate Hog1. Due to this constraint, newer mass spectrometry strategies involve using kinase inhibitors together with machine learning techniques to address some of these limitations [121]. In addition, it was found that abundance did not affect the time at which significant FC ($FC_{max}/2$) occurred. Thus, it led to us to conclude that KPs and their substrate have enough specificity, and that less abundant KPs were also regulated within the first minute of the 0-33 minute timescale.

This study has made it possible to start contemplating the link between signaling rates and the kinetics of phosphopeptides during osmoadaptation. Linking phosphorylation kinetics to biological traits can have profound consequences in our understanding of how

a cell functions. For example, comparing the phosphorylation kinetics between the two osmosensing branches, Sho1 and Sln1, and projecting these kinetics to other features such as signal fidelity, robustness and responsiveness is a substantial task. To this end, much work is still required. This includes the verification of the kinetic phosphosites found in this study, capturing other phosphopeptides that were lost due to using trypsin digestion, capturing other phosphorylation events such as Sln1p-Ypd1-Ssk1p two-component system, and also maximizing the mono-phosphorylated peptides, which would in turn yield higher data quality.

The phosphoproteomic analysis has found 24% (31/129) of kinases and 10% of phosphatases (3/30) to have a dynamic profile within the sub-minute timescale. And on the half-hour timescale, 33% of kinases (43/129) and 10% of phosphatases (3/30) revealed a dynamic profile. The KPs that had these kinetic profiles are highly interconnected, creating a dense interwoven interaction network. The most connected node in the sub-minute timescale was Hog1. However, this was replaced by Cdc28 in the longer timescale (Figure 15). This could be indicative of how cells adapt to high osmolarity over time. Moreover, gene ontology on the 100 protein that have seen regulation on both timescales revealed an enrichment of GO terms such as cellular bud neck, cytoplasmic mRNA processing body, endocytosis, negative regulation of translation (Figure 18). Finally, adding in account of the continuity measured in these kinetic profiles for peptides undergoing phosphorylation or dephosphorylation, SILAC coupled to LC-MS/MS is probably one of the best stimuli-specific high-throughput method for predicting functional phosphosites in cells.

References

[1]   S. Hohmann, "Osmotic Stress Signaling and Osmoadaptation in Yeasts," *Microbiol. Mol. Biol. Rev.*, vol. 66, no. 2, pp. 300–372, 2003.

[2]   A. D. Sharrocks, S. H. Yang, and A. Galanis, "Docking domains and substrate-specificity determination for MAP kinases," *Trends in Biochemical Sciences*, vol. 25, no. 9. pp. 448–453, 2000.

[3]   J. E. Hallsworth, Y. Nomura, and M. Iwahara, "Ethanol-induced water stress and fungal growth," *J. Ferment. Bioeng.*, vol. 86, no. 5, pp. 451–456, 1998.

[4]   P. W. Piper, "The heat shock and ethanol stress responses of yeast exhibit extensive similarity and functional overlap," *FEMS Microbiology Letters*, vol. 134, no. 2–3. pp. 121–127, 1995.

[5]   J. L. Brewster, T. De Valoir, N. D. Dwyer, E. Winter, and M. C. Gustin, "An osmosensing signal transduction pathway in yeast," *Science (80-.).*, vol. 259, no. 5102, pp. 1760–1763, 1993.

[6]   M. W. Covert, C. H. Schilling, and B. Palsson, "Regulation of gene expression in flux balance models of metabolism," *J. Theor. Biol.*, vol. 213, no. 1, pp. 73–88, 2001.

[7]   B. C. Berk, R. J. Ulevitch, J. Abe, M. Kusuhara, and J.-D. Lee, "Big Mitogen-activated Protein Kinase 1 (BMK1) Is a Redox-sensitive Kinase," *J. Biol. Chem.*, vol. 271, no. 28, pp. 16586–16590, 2002.

[8]   S. M. Wurgler-Murphy, T. Maeda, E. a Witten, and H. Saito, "Regulation of the Saccharomyces cerevisiae HOG1 mitogen-activated protein kinase by the PTP2 and PTP3 protein tyrosine phosphatases.," *Mol. Cell. Biol.*, vol. 17, no. 3, pp. 1289–1297, 1997.

[9]   V. Reiser, H. Ruis, and G. Ammerer, "Kinase activity-dependent nuclear export opposes stress-induced nuclear accumulation and retention of Hog1 mitogen-activated protein kinase in the budding yeast Saccharomyces cerevisiae.," *Mol. Biol. Cell*, vol. 10, no. 4, pp. 1147–1161, 1999.

[10]   H. Saito and F. Posas, "Response to hyperosmotic stress," *Genetics*, vol. 192, no. 2. pp. 289–318, 2012.

[11]   T. Maeda, M. Takekawa, and H. Saito, "Activation of yeast PBS2 MAPKK by MAPKKKs or by binding of an SH3-containing osmosensor," *Science (80-.).*, vol. 269, no. 5223, pp. 554–558, 1995.

[12]   I. M. Ota and A. Varshavsky, "A yeast protein similar to bacterial two-component regulators," *Science (80-.).*, vol. 262, no. 5133, pp. 566–569, 1993.

[13]   A. M. Stock and V. L. Robinson, "Two-component signal transduction," *Annu. Rev. …*, vol. 69, pp. 183–215, 2000.

[14]   T. Maeda, S. M. Wurgler-Murphy, and H. Saito, "A two-component system that regulates an osmosensing MAP kinase cascade in yeast," *Nature*, vol. 369, no. 6477, pp. 242–245, 1994.

[15]   J. L. Brewster and M. C. Gustin, "Hog1: 20 years of discovery and impact," *Science Signaling*, vol. 7, no. 343. 2014.

[16]   B. Birkaya, A. Maddi, J. Joshi, S. J. Free, and P. J. Cullen, "Role of the cell wall integrity and filamentous growth mitogen-activated protein kinase pathways in cell

wall remodeling during filamentous growth," *Eukaryot. Cell*, vol. 8, no. 8, pp. 1118–1133, 2009.

[17]   I. Maayan and D. Engelberg, "The yeast MAPK Hog1 is not essential for immediate survival under osmostress," *FEBS Lett.*, vol. 583, no. 12, pp. 2015–2020, 2009.

[18]   J. Albertyn, S. Hohmann, J. M. Thevelein, and B. A. Prior, "GPD1, which encodes glycerol-3-phosphate dehydrogenase, is essential for growth under osmotic stress in Saccharomyces cerevisiae, and its expression is regulated by the high-osmolarity glycerol response pathway.," *Mol. Cell. Biol.*, vol. 14, no. 6, pp. 4135–4144, 2015.

[19]   J. Norbeck, A. K. Påhlman, N. Akhtar, A. Blomberg, and L. Adler, "Purification and characterization of two isoenzymes of DL-glycerol-3-phosphatase from Saccharomyces cerevisiae: Identification of the corresponding GPP1 and GPP2 genes and evidence for osmotic regulation of Gpp2p expression by the osmosensing mitogen-acti," *J. Biol. Chem.*, vol. 271, no. 23, pp. 13875–13881, 1996.

[20]   J. Yale and H. J. Bohnert, "Transcript Expression in Saccharomyces cerevisiae at High Salinity," *J. Biol. Chem.*, vol. 276, no. 19, pp. 15996–16007, 2001.

[21]   E. S. Lander, S. S. Koh, R. A. Young, C. T. Harbison, T. I. Lee, E. G. Jennings, H. L. True, B. Ren, H. C. Causton, and E. Kanin, "Remodeling of Yeast Genome Expression in Response to Environmental Changes," *Mol. Biol. Cell*, vol. 12, no. 2, pp. 323–337, 2013.

[22]   A. P. Schmitt and K. McEntee, "Msn2p, a zinc finger DNA-binding protein, is the transcriptional activator of the multistress response in Saccharomyces cerevisiae.," *Proc. Natl. Acad. Sci. U. S. A.*, vol. 93, no. 12, pp. 5777–82, 1996.

[23]   T. Beck and M. N. Hall, "The TOR signalling pathway controls nuclear localization of nutrient- regulated transcription factors," *Nature*, vol. 402, no. 6762, pp. 689–692, 1999.

[24]   F. Estruch, G. Ammerer, M. T. Martinez-Pastor, E. Durchschlag, B. Hamilton, C. Schuller, W. Gorner, and H. Ruis, "Nuclear localization of the C2H2 zinc finger protein Msn2p is regulated by stress and protein kinase A activity," *Genes Dev.*, vol. 12, no. 4, pp. 586–597, 2008.

[25]   P. Kubiniok, D. D'Amours, P. Thibault, Y. Thattikota, and E. Kanshin, "Phosphoproteome dynamics of Saccharomyces cerevisiae under heat shock and cold stress," *Mol. Syst. Biol.*, vol. 11, no. 6, pp. 813–813, 2015.

[26]   E. Kanshin, L. P. Bergeron-Sandoval, S. S. Isik, P. Thibault, and S. W. Michnick, "A Cell-Signaling Network Temporally Resolves Specific versus Promiscuous Phosphorylation," *Cell Rep.*, vol. 10, no. 7, pp. 1202–1214, 2015.

[27]   J. Lee, W. Reiter, I. Dohnal, C. Gregori, S. Beese-Sims, K. Kuchler, G. Ammerer, and D. E. Levin, "MAPK Hog1 closes the S. cerevisiae glycerol channel Fps1 by phosphorylating and displacing its positive regulators," *Genes Dev.*, 2013.

[28]   R. Babazadeh, T. Furukawa, S. Hohmann, and K. Furukawa, "Rewiring yeast osmostress signalling through the MAPK network reveals essential and non-essential roles of Hog1 in osmoadaptation," *Sci. Rep.*, vol. 4, 2014.

[29]   E. Bilsland-Marchesan, J. Ariño, H. Saito, P. Sunnerhagen, and F. Posas, "Rck2 kinase is a substrate for the osmotic stress-activated mitogen-activated protein kinase Hog1.," *Mol. Cell. Biol.*, vol. 20, no. 11, pp. 3887–95, 2000.

[30]   T. Prick, M. Thumm, D. Häussinger, and S. Vom Dahl, "Deletion of HOG1 leads to osmosensitivity in starvation-induced, but not rapamycin-dependent Atg8 degradation and proteolysis: Further evidence for different regulatory mechanisms

in yeast autophagy," *Autophagy*, vol. 2, no. 3. pp. 241–243, 2006.

[31]   G. R. Jeschke, F. M. Roelants, Y. J. Lee, B. E. Turk, and J. Thorner, "Reciprocal Phosphorylation of Yeast Glycerol-3-Phosphate Dehydrogenases in Adaptation to Distinct Types of Stress," *Mol. Cell. Biol.*, vol. 32, no. 22, pp. 4705–4717, 2012.

[32]   A. Muir, S. Ramachandran, F. M. Roelants, G. Timmons, and J. Thorner, "TORC2-dependent protein kinase Ypk1 phosphorylates ceramide synthase to stimulate synthesis of complex sphingolipids," *Elife*, vol. 3, 2014.

[33]   A. Muir, F. M. Roelants, G. Timmons, K. L. Leskoske, and J. Thorner, "Down-regulation of TORC2-Ypk1 signaling promotes MAPK-independent survival under hyperosmotic stress," *Elife*, vol. 4, no. AUGUST2015, 2015.

[34]   A. A. Granados, M. M. Crane, L. F. Montano-Gutierrez, R. J. Tanaka, M. Voliotis, and P. S. Swain, "Distributing tasks via multiple input pathways increases cellular survival in stress," *Elife*, vol. 6, 2017.

[35]   K. M. Schmoller, J. J. Turner, M. Kõivomägi, and J. M. Skotheim, "Dilution of the cell cycle inhibitor Whi5 controls budding-yeast cell size," *Nature*, vol. 526, no. 7572, pp. 268–272, 2015.

[36]   S. J. Elledge, "Cell cycle checkpoints: Preventing an identity crisis," *Science (80-.).*, vol. 274, no. 5293, pp. 1664–1672, 1996.

[37]   G. Bellí, E. Garí, M. Aldea, and E. Herrero, "Osmotic stress causes a G1 cell cycle delay and downregulation of Cln3/Cdc28 activity in Saccharomyces cerevisiae," *Mol. Microbiol.*, vol. 39, no. 4, pp. 1022–1035, 2001.

[38]   N. F. Lowndes, A. L. Johnson, and L. H. Johnston, "Coordination of expression of DNA synthesis genes in budding yeast by a cell-cycle regulated trans factor," *Nature*, vol. 350, no. 6315, pp. 247–250, 1991.

[39]   B. J. Andrews and I. Herskowitz, "Identification of a DNA binding factor involved in cell-cycle control of the yeast HO gene," *Cell*, vol. 57, no. 1, pp. 21–29, 1989.

[40]   M. R. M. Taba, I. Muroff, D. Lydall, G. Tebb, and K. Nasmyth, "Changes in a SWI4,6-DNA-binding complex occur at the time of HO gene activation in yeast," *Genes Dev.*, vol. 5, no. 11, pp. 2000–2013, 1991.

[41]   M. Costanzo, J. L. Nishikawa, X. Tang, J. S. Millman, O. Schub, K. Breitkreuz, D. Dewar, I. Rupes, B. Andrews, and M. Tyers, "CDK activity antagonizes Whi5, an inhibitor of G1/S transcription in yeast," *Cell*, vol. 117, no. 7, pp. 899–913, 2004.

[42]   R. A. M. De Bruin, W. H. McDonald, T. I. Kalashnikova, J. Yates, and C. Wittenberg, "Cln3 activates G1-specific transcription via phosphorylation of the SBF bound repressor Whi5," *Cell*, vol. 117, no. 7, pp. 887–898, 2004.

[43]   D. Heinegård and Y. Sommarin, "[17] Isolation and characterization of proteoglycans," *Genetics*, pp. 319–372, 2004.

[44]   R. Sopko, D. Huang, N. Preston, G. Chua, B. Papp, K. Kafadar, M. Snyder, S. G. Oliver, M. Cyert, T. R. Hughes, C. Boone, and B. Andrews, "Mapping pathways and phenotypes by systematic gene overexpression," *Mol. Cell*, vol. 21, no. 3, pp. 319–330, 2006.

[45]   N. Bastajian, H. Friesen, and B. J. Andrews, "Bck2 Acts through the MADS Box Protein Mcm1 to Activate Cell-Cycle-Regulated Genes in Budding Yeast," *PLoS Genet.*, vol. 9, no. 5, 2013.

[46]   C. J. Di Como, H. Chang, and K. T. Arndt, "Activation of CLN1 and CLN2 G1 cyclin gene expression by BCK2.," *Mol. Cell. Biol.*, vol. 15, no. 4, pp. 1835–1846, 2015.

[47]   J. Cieśla, T. Frączyk, and W. Rode, "Phosphorylation of basic amino acid residues in proteins," *Acta Biochim. Pol.*, vol. 58, no. 2. 2011.

[48]   G. E. Lienhard, "Non-functional phosphorylations?," *Trends Biochem. Sci.*, vol. 33,

no. 8, pp. 351–352, Aug. 2008.

[49]   C. R. Landry, E. D. Levy, and S. W. Michnick, "Weak functional constraints on phosphoproteomes," *Trends in Genetics*, vol. 25, no. 5. pp. 193–197, 2009.

[50]   D. S. Tawfik, "Messy biology and the origins of evolutionary innovations," *Nature Chemical Biology*. 2010.

[51]   G. Manning, D. B. Whyte, R. Martinez, T. Hunter, and S. Sudarsanam, "The protein kinase complement of the human genome," *Science*, vol. 298, no. 5600. pp. 1912–1934, 2002.

[52]   E. D. Levy, S. W. Michnick, and C. R. Landry, "Protein abundance is key to distinguish promiscuous from functional phosphorylation based on evolutionary information," *Philosophical Transactions of the Royal Society B: Biological Sciences*, vol. 367, no. 1602. pp. 2594–2606, 2012.

[53]   G. Liu, M. Tyers, L. Boucher, B. Larsen, A. C. Gingras, J. Ahn, A. I. Nesvizhskii, T. Reguly, H. Choi, D. Dewar-Darch, V. Neduva, C. Stark, X. Tang, T. Pawson, A. Breitkreutz, J. R. Sharom, B. J. Breitkreutz, Z. Y. Lin, Z. S. Qin, and R. Almeida, "A Global Protein Kinase and Phosphatase Interaction Network in Yeast," *Science (80-.).*, vol. 328, no. 5981, pp. 1043–1046, 2010.

[54]   S. Wanka, B. Bodenmiller, B. Gerrits, J. Urban, A. I. Nesvizhskii, M. Peter, O. Vitek, R. Schlapbach, B. Roschitzki, R. Aebersold, H. Lam, K. M. Shokat, P. Picotti, M.-Y. Brusniak, C. von Mering, R. Loewith, C. Zhang, A. Colman-Lerner, D. Campbell, P. G. Pedrioli, C. Kraft, and G. P. Nolan, "Phosphoproteomic Analysis Reveals Interconnected System-Wide Responses to Perturbations of Kinases and Phosphatases in Yeast," *Sci. Signal.*, vol. 3, no. 153, pp. rs4-rs4, 2010.

[55]   N. Yachie, R. Saito, N. Sugiyama, M. Tomita, and Y. Ishihama, "Integrative features of the yeast phosphoproteome and protein-protein interaction map," *PLoS Comput. Biol.*, vol. 7, no. 1, 2011.

[56]   Z. Wang, G. Ding, L. Geistlinger, H. Li, L. Liu, R. Zeng, Y. Tateno, and Y. Li, "Evolution of protein phosphorylation for distinct functional modules in vertebrate genomes," *Mol. Biol. Evol.*, vol. 28, no. 3, pp. 1131–1140, 2011.

[57]   C. Jorgensen, B. Bodenmiller, G. D. Bader, R. Aebersold, M. Jovanovic, C. S. H. Tan, A. Pasculescu, M. O. Hengartner, T. Pawson, and R. Linding, "Comparative Analysis Reveals Conserved Protein Phosphorylation Networks Implicated in Multiple Diseases," *Sci. Signal.*, vol. 2, no. 81, pp. ra39-ra39, 2009.

[58]   A. N. Nguyen Ba and A. M. Moses, "Evolution of characterized phosphorylation sites in budding yeast," *Mol. Biol. Evol.*, vol. 27, no. 9, pp. 2027–2037, 2010.

[59]   R. Malik, E. A. Nigg, and R. Körner, "Comparative conservation analysis of the human mitotic phosphoproteome," *Bioinformatics*, vol. 24, no. 12, pp. 1426–1432, 2008.

[60]   R. Wu, W. Haas, N. Dephoure, E. L. Huttlin, B. Zhai, M. E. Sowa, and S. P. Gygi, "A large-scale method to measure absolute protein phosphorylation stoichiometries," *Nat. Methods*, vol. 8, no. 8, pp. 677–683, 2011.

[61]   A. Pasculescu, J. G. Park, L. J. Jensen, K. Colwill, I. M. Miron, P. Metalnikov, P. Bork, K. Elder, C. Jørgensen, L. D. Samson, F. Diella, M. A. T. M. van Vugt, M. B. Yaffe, T. Pawson, L. Taylor, R. Linding, J. R. Woodgett, R. B. Russell, G. J. Ostheimer, V. Nguyen, and J. Jin, "Systematic Discovery of In Vivo Phosphorylation Networks," *Cell*, vol. 129, no. 7, pp. 1415–1426, 2007.

[62]   G. Chechik, A. C. Silva, M. Shales, G. Cagney, J. S. Weissman, F. C. P. Holstege, S. van Wageningen, K. M. Shokat, N. J. Krogan, S. R. Collins, M. Mehta, H. Braberg, D. Fiedler, P. Mukherjee, P. Kemmeren, D. Koller, and M.-C. Keogh,

"Functional Organization of the S. cerevisiae Phosphorylation Network," *Cell*, vol. 136, no. 5, pp. 952–963, 2009.

[63]   H. Zhu, M. J. R. Stark, C. De Virgilio, B. Schweitzer, N. Rachidi, M. Snyder, H. Guo, D. F. Stern, G. Devgan, J. Fasolo, P. F. Predki, X. Zhu, M. C. Schmidt, B. Andrews, A. S. Mah, S.-J. Lee, A. Breitkreutz, G. Michaud, L. Meng, R. R. McCartney, R. Sopko, G. Jona, M. Tyers, J. Ptacek, and M. Gerstein, "Global analysis of protein phosphorylation in yeast," *Nature*, vol. 438, no. 7068, pp. 679–684, 2005.

[64]   C. Cheng, E. Andrews, K. K. Yan, M. Ung, D. Wang, and M. Gerstein, "An approach for determining and measuring network hierarchy applied to comparing the phosphorylome and the regulome," *Genome Biol.*, vol. 16, no. 1, 2015.

[65]   D. Abd-Rabbo and S. W. Michnick, "Delineating functional principles of the bow tie structure of a kinase-phosphatase network in the budding yeast," *BMC Syst. Biol.*, vol. 11, no. 1, pp. 1–14, 2017.

[66]   J. S. Weissman, J. L. DeRisi, D. K. Breslow, M. Noble, J. R. S. Newman, S. Ghaemmaghami, and J. Ihmels, "Single-cell proteomic analysis of S. cerevisiae reveals the architecture of biological noise," *Nature*, vol. 441, no. 7095, pp. 840–846, 2006.

[67]   M. R. Di Falco, "Mass spectrometry-based proteomics," *Methods in Molecular Biology*, vol. 1775. pp. 93–106, 2018.

[68]   F. Lemi, "Interfaces for LC – MS Accelerating electrode," *Guid. to LC-MS*, no. December, pp. 21–27, 2001.

[69]   J. B. Fenn, M. Mann, C. K. Meng, S. F. Wong, and C. M. Whitehouse, "Electrospray ionization for mass spectrometry of large biomolecules," *Science (80-.).*, vol. 246, no. 4926, pp. 64–71, 1989.

[70]   A. Matta, R. Ralhan, L. V. Desouza, and K. W. M. Siu, *Mass spectrometry-based clinical proteomics: Head-and-neck cancer biomarkers and drug-targets discovery*, vol. 29, no. 6. 2010.

[71]   S. Eliuk and A. Makarov, "Evolution of Orbitrap Mass Spectrometry Instrumentation," *Annu. Rev. Anal. Chem.*, vol. 8, no. 1, pp. 61–80, 2015.

[72]   Fred W. McLafferty, I. Jonathan Amster, Jorge J. P. Furlong, Joseph A. Loo, Bing H. Wang, and Evan R. Williams, "Fourier Transform Mass Spectrometry," *Mol. Cell. Proteomics*, vol. 359, pp. 116–126, 1987.

[73]   J. J. Pitt, "Principles and applications of liquid chromatography-mass spectrometry in clinical biochemistry.," *Clin. Biochem. Rev.*, 2009.

[74]   B. Blagoev, M. Mann, D. B. Kristensen, H. Steen, I. Kratchmarova, S.-E. Ong, and A. Pandey, "Stable Isotope Labeling by Amino Acids in Cell Culture, SILAC, as a Simple and Accurate Approach to Expression Proteomics," *Mol. Cell. Proteomics*, vol. 1, no. 5, pp. 376–386, 2003.

[75]   E. Kanshin, S. W. Michnick, and P. Thibault, "Displacement of N/Q-rich peptides on TiO2 beads enhances the depth and coverage of yeast phosphoproteome analyses," *J. Proteome Res.*, vol. 12, no. 6, pp. 2905–2913, 2013.

[76]   J. Rappsilber, Y. Ishihama, and M. Mann, "Stop And Go Extraction tips for matrix-assisted laser desorption/ionization, nanoelectrospray, and LC/MS sample pretreatment in proteomics," *Anal. Chem.*, vol. 75, no. 3, pp. 663–670, 2003.

[77]   Y. Ishihama, J. Rappsilber, and M. Mann, "Modular stop and go extraction tips with stacked disks for parallel and multidimensional peptide fractionation in proteomics," *J. Proteome Res.*, vol. 5, no. 4, pp. 988–994, 2006.

[78]   J. Cox and M. Mann, "MaxQuant enables high peptide identification rates,

individualized p.p.b.-range mass accuracies and proteome-wide protein quantification," *Nat. Biotechnol.*, vol. 26, no. 12, pp. 1367–1372, 2008.

[79] J. Cox, A. Michalski, and M. Mann, "Software lock mass by two-dimensional minimization of peptide mass errors," *J. Am. Soc. Mass Spectrom.*, vol. 22, no. 8, pp. 1373–1380, 2011.

[80] K. Willbrand, F. Radvanyi, J. P. Nadal, J. P. Thiery, and T. M. A. Fink, "Identifying genes from up-down properties of microarray expression series," *Bioinformatics*, 2005.

[81] G. G. Szpiro, "The number of permutations with a given signature, and the expectations of their elements," *Discrete Math.*, vol. 226, no. 1–3, pp. 423–430, 2001.

[82] M. E. FUTSCHIK and B. CARLISLE, "Noise-Robust Soft Clustering of Gene Expression Time-Course Data," *J. Bioinform. Comput. Biol.*, vol. 03, no. 04, pp. 965–988, 2005.

[83] R. Nock and F. Nielsen, "On weighting clustering," *IEEE Trans. Pattern Anal. Mach. Intell.*, vol. 28, no. 8, pp. 1223–1235, 2006.

[84] L. Kumar and M. E. Futschik, "Mfuzz: A software package for soft clustering of microarray data," *Bioinformation*, vol. 2, no. 1, pp. 5–7, 2012.

[85] V. Schwämmle and O. N. Jensen, "A simple and fast method to determine the parameters for fuzzy c-means cluster analysis," *Bioinformatics*, vol. 26, no. 22, pp. 2841–2848, 2010.

[86] B. Breitkreutz, C. Stark, and M. Tyers, "The GRID: the General Repository for Interaction Datasets," *Genome Biol.*, vol. 4, no. 3, p. R23, 2002.

[87] A. Chatr-Aryamontri, R. Oughtred, L. Boucher, J. Rust, C. Chang, N. K. Kolas, L. O'Donnell, S. Oster, C. Theesfeld, A. Sellam, C. Stark, B. J. Breitkreutz, K. Dolinski, and M. Tyers, "The BioGRID interaction database: 2017 update," *Nucleic Acids Res.*, vol. 45, no. D1, pp. D369–D379, 2017.

[88] J. Lin, P. Bork, L. J. Jensen, D. Szklarczyk, M. Simonovic, S. Frankild, C. von Mering, A. Franceschini, A. Roth, P. Minguez, and M. Kuhn, "STRING v9.1: protein-protein interaction networks, with increased coverage and integration," *Nucleic Acids Res.*, vol. 41, no. D1, pp. D808–D815, 2012.

[89] I. Shames, Y. Malitskaya, H. Bussey, S. Radinovic, M. M. S. Molina, S. W. Michnick, K. Tarassov, C. R. Landry, J. Vogel, and V. Messier, "An in Vivo Map of the Yeast Protein Interactome," *Science (80-.).*, vol. 320, no. 5882, pp. 1465–1470, 2008.

[90] A. Chatr-Aryamontri, B. J. Breitkreutz, S. Heinicke, L. Boucher, A. Winter, C. Stark, J. Nixon, L. Ramage, N. Kolas, L. O'Donnell, T. Reguly, A. Breitkreutz, A. Sellam, D. Chen, C. Chang, J. Rust, M. Livstone, R. Oughtred, K. Dolinski, and M. Tyers, "The BioGRID interaction database: 2013 Update," *Nucleic Acids Res.*, vol. 41, no. D1, 2013.

[91] D. W. Huang, B. T. Sherman, and R. A. Lempicki, "Systematic and integrative analysis of large gene lists using DAVID bioinformatics resources," *Nat. Protoc.*, vol. 4, no. 1, pp. 44–57, 2009.

[92] D. W. Huang, B. T. Sherman, and R. A. Lempicki, "Bioinformatics enrichment tools: Paths toward the comprehensive functional analysis of large gene lists," *Nucleic Acids Res.*, vol. 37, no. 1, pp. 1–13, 2009.

[93] T. Grevesse, B. E. Dabiri, K. K. Parker, and S. Gabriele, "Opposite rheological properties of neuronal microcompartments predict axonal vulnerability in brain injury," *Sci. Rep.*, vol. 5, 2015.

[94] S. E. Ong and M. Mann, "A practical recipe for stable isotope labeling by amino acids in cell culture (SILAC)," *Nat. Protoc.*, 2006.

[95] H. C. Harsha, H. Molina, and A. Pandey, "Quantitative proteomics using stable isotope labeling with amino acids in cell culture.," *Nat. Protoc.*, vol. 3, no. 3, pp. 505–16, 2008.

[96] F. Posas, S. M. Wurgler-Murphy, T. Maeda, E. A. Witten, T. C. Thai, and H. Saito, "Yeast HOG1 MAP kinase cascade is regulated by a multistep phosphorelay mechanism in the SLN1-YPD1-SSK1 'two-component' osmosensor," *Cell*, vol. 86, no. 6, pp. 865–875, 1996.

[97] K. Tanaka, K. Tatebayashi, A. Nishimura, K. Yamamoto, H. Y. Yang, and H. Saito, "Yeast osmosensors Hkr1 and Msb2 activate the Hog1 MAPK cascade by different mechanisms," *Sci. Signal.*, 2014.

[98] K. Yamamoto, K. Tatebayashi, K. Tanaka, and H. Saito, "Dynamic control of yeast MAP kinase network by induced association and dissociation between the ste50 scaffold and the Opy2 membrane anchor," *Mol. Cell*, vol. 40, no. 1, pp. 87–98, 2010.

[99] N. V. Varlakhanova, M. J. Mihalevic, K. A. Bernstein, and M. G. J. Ford, "Pib2 and the EGO complex are both required for activation of TORC1," *J. Cell Sci.*, vol. 130, no. 22, pp. 3878–3890, 2017.

[100] Y. Cai and B. Futcher, "Effects of the yeast RNA-binding protein Whi3 on the half-life and abundance of CLN3 mRNA and other targets," *PLoS One*, vol. 8, no. 12, 2013.

[101] C. Lee, H. Zhang, A. E. Baker, P. Occhipinti, M. E. Borsuk, and A. S. Gladfelter, "Protein Aggregation Behavior Regulates Cyclin Transcript Localization and Cell-Cycle Control," *Dev. Cell*, vol. 25, no. 6, pp. 572–584, 2013.

[102] E. Garí, T. Volpe, H. Wang, C. Gallego, B. Futcher, and M. Aldea, "Whi3 binds the mRNA of the G1 cyclin CLN3 to modulate cell fate in budding yeast," *Genes Dev.*, vol. 15, no. 21, pp. 2803–2808, 2001.

[103] E. de Nadal, M. Nadal-Ribelles, J. Jiménez, S. Cavero, J. Clotet, F. Posas, and A. González-Novo, "Hog1 Targets Whi5 and Msa1 Transcription Factors To Downregulate Cyclin Expression upon Stress," *Mol. Cell. Biol.*, vol. 35, no. 9, pp. 1606–1618, 2015.

[104] M. V. Wagner, M. B. Smolka, R. A. M. de Bruin, H. Zhou, C. Wittenberg, and S. F. Dowdy, "Whi5 regulation by site specific CDK-phosphorylation in Saccharomyces cerevisiae," *PLoS One*, 2009.

[105] A. S. Gladfelter, C. Lee, M. E. Borsuk, A. E. Baker, H. Zhang, and P. Occhipinti, "Protein Aggregation Behavior Regulates Cyclin Transcript Localization and Cell-Cycle Control," *Dev. Cell*, vol. 25, no. 6, pp. 572–584, 2013.

[106] D. L. Swaney, P. Beltrao, L. Starita, A. Guo, J. Rush, S. Fields, N. J. Krogan, and J. Villén, "Global analysis of phosphorylation and ubiquitylation cross-talk in protein degradation," *Nat. Methods*, vol. 10, no. 7, pp. 676–682, 2013.

[107] B. Andrews, J. Haynes, J. Moffat, K. Baetz, and M. Chang, "Transcriptional Coregulation by the Cell Integrity Mitogen-Activated Protein Kinase Slt2 and the Cell Cycle Regulator Swi4," *Mol. Cell. Biol.*, vol. 21, no. 19, pp. 6515–6528, 2002.

[108] C. von Mering, S. P. Schrimpf, M. Wang, M. Weiss, M. O. Hengartner, M. Simonovic, and G. Haertinger, "PaxDb, a Database of Protein Abundance Averages Across All Three Domains of Life," *Mol. Cell. Proteomics*, vol. 11, no. 8, pp. 492–500, 2012.

[109] L. Magtanong, R. J. Andersen, J. Porter, S. L. Barker, C. Nislow, C. Boone, M.

Yoshida, J. L. Y. Koh, T. R. Graham, G. Giaever, D. Gresham, B. Andrews, S. Nishimura, C. H. Ho, D. Botstein, P. Natarajan, and C. A. Gray, "A molecular barcoded yeast ORF library enables mode-of-action analysis of bioactive compounds," *Nat. Biotechnol.*, vol. 27, no. 4, pp. 369–377, 2009.

[110] J. E. Hughes Hallett, X. Luo, and A. P. Capaldi, "State transitions in the TORC1 signaling pathway and information processing in Saccharomyces cerevisiae," *Genetics*, vol. 198, no. 2, pp. 773–786, 2014.

[111] G. Ammerer, D. Mukhopadhyay, J. R. Broach, H. Riezman, A. Soulard, R. Loewith, J. Urban, S. Lippman, D. Anrather, C. De Virgilio, A. Huber, V. Wanke, O. Deloche, and M. N. Hall, "Sch9 Is a Major Target of TORC1 in Saccharomyces cerevisiae," *Mol. Cell*, vol. 26, no. 5, pp. 663–674, 2007.

[112] C. Arkind, A. Burkholder, I. Ota, K. Knoche, A. Winkler, and C. P. Mattison, "Heat Stress Activates the Yeast High-Osmolarity Glycerol Mitogen-Activated Protein Kinase Pathway, and Protein Tyrosine Phosphatases Are Essential under Heat Stress," *Eukaryot. Cell*, vol. 1, no. 2, pp. 163–173, 2002.

[113] A. Huber, S. L. French, H. Tekotte, S. Yerlikaya, M. Stahl, M. P. Perepelkina, M. Tyers, J. Rougemont, A. L. Beyer, and R. Loewith, "Sch9 regulates ribosome biogenesis via Stb3, Dot6 and Tod6 and the histone deacetylase complex RPD3L," *EMBO J.*, vol. 30, no. 15, p. 3052 LP-3064, Aug. 2011.

[114] B. T. McDaniel and J. S. Radesky, "Technoference: Parent Distraction With Technology and Associations With Child Behavior Problems," *Child Dev.*, vol. 89, no. 1, pp. 100–109, 2018.

[115] J. Lee, R. D. Moir, and I. M. Willis, "Regulation of RNA Polymerase III Transcription Involves SCH9-dependent and SCH9-independent Branches of the Target of Rapamycin (TOR) Pathway," *J. Biol. Chem.*, vol. 284, no. 19, pp. 12604–12608, May 2009.

[116] W. Krek and E. A. Nigg, "Mutations of p34cdc2 phosphorylation sites induce premature mitotic events in HeLa cells: evidence for a double block to p34cdc2 kinase activation in vertebrates.," *EMBO J.*, vol. 10, no. 11, pp. 3331–3341, 2018.

[117] C. Norbury, J. Blow, and P. Nurse, "Regulatory phosphorylation of the p34cdc2 protein kinase in vertebrates.," *EMBO J.*, vol. 10, no. 11, pp. 3321–3329, 2018.

[118] G. J. Den Haese, N. Walworth, A. M. Carr, and K. L. Gould, "The Wee1 protein kinase regulates T14 phosphorylation of fission yeast Cdc2.," *Mol. Biol. Cell*, vol. 6, no. 4, pp. 371–385, 2013.

[119] M. A. Soliman, A.-C. Gingras, L. Taylor, R. J. Daly, N. St-Denis, A. Y. Dai, T. Pawson, A. Pasculescu, R. Bagshaw, Y. Zheng, K. Colwill, S. A. Tate, C. Zhang, J. W. Dennis, D. R. Croucher, and W. R. Hardy, "Temporal regulation of EGF signalling networks by the scaffold protein Shc1," *Nature*, vol. 499, no. 7457, pp. 166–171, 2013.

[120] R. P. Bhattacharyya, A. Reményi, B. J. Yeh, and W. A. Lim, "Domains, Motifs, and Scaffolds: The Role of Modular Interactions in the Evolution and Wiring of Cell Signaling Circuits," *Annu. Rev. Biochem.*, vol. 75, no. 1, pp. 655–680, 2006.

[121] E. Kanshin, S. Giguère, P. Thibault, C. Jing, and M. Tyers, "Machine Learning of Global Phosphoproteomic Profiles Enables Discrimination of Direct versus Indirect Kinase Substrates," *Mol. Cell. Proteomics*, vol. 16, no. 5, pp. 786–798, 2017.

[122] H. Yurimoto, Y. Sakai, T. Hioki, A. Habata, and K. Shiraishi, "Yeast Hog1 proteins are sequestered in stress granules during high-temperature stress," *J. Cell Sci.*, vol. 131, no. 1, p. jcs209114, 2017.